International Journal of Pharmaceutics 657 (2024) 124136

Contents lists available at ScienceDirect

International Journal of Pharmaceutics

journal homepage: www.elsevier.com/locate/ijpharm

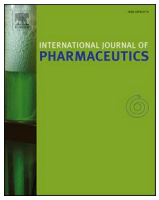

Antimicrobial liposomes-in-nanofiber wound dressings prepared by a green and sustainable wire-electrospinning set-up

Laura Victoria Schulte-Werning [a], Bhupender Singh [b], Mona Johannessen [b], Rolf Einar Engstad [c], Ann Mari Holsæter [a,*]

[a] Drug Transport and Delivery Research Group, Department of Pharmacy, Faculty of Health Sciences, UiT The Arctic University of Norway, 9037 Tromsø, Norway
[b] Research Group for Host-Microbe Interaction, Department of Medical Biology, Faculty of Health Sciences, UiT The Arctic University of Norway, 9037 Tromsø, Norway
[c] Biotec BetaGlucans AS, 9019 Tromsø, Norway

ARTICLE INFO

Keywords:
Wire-electrospinning
Liposomes in nanofibers
Chloramphenicol
Wound dressing
Chronic wounds
Elmarco Nanospider™

ABSTRACT

Increasing prevalence of infected and chronic wounds demands improved therapy options. In this work an electrospun nanofiber dressing with liposomes is suggested, focusing on the dressing's ability to support tissue regeneration and infection control. Chloramphenicol (CAM) was the chosen antibiotic, added to the nanofibers after first embedded in liposomes to maintain a sustained drug release. Nanofibers spun from five different polymer blends were tested, where pectin and polyethylene oxide (PEO) was identified as the most promising polymer blend, showing superior fiber formation and tensile strength. The wire-electrospinning setup (WES) was selected for its pilot-scale features, and water was applied as the only solvent for green electrospinning and to allow direct liposome incorporation. CAM-liposomes were added to Pectin-PEO nanofibers in the next step. Confocal imaging of rhodamine-labelled liposomes indicated intact liposomes in the fibers after electrospinning. This was supported by the observed *in vitro* CAM-release, showing that Pectin-PEO-nanofibers with CAM-liposomes had a delayed drug release compared to controls. Biological testing confirmed the antimicrobial efficacy of CAM and good biocompatibility of all CAM-nanofibers. The successful fiber formation and green production process with WES gives a promising outlook for industrial upscaling.

1. Introduction

With an aging population and rising incidence of diabetes and obesity, chronic wounds represent a significant and global societal economic burden. Chronic wounds are causing pain and medical harm, which not only affect patients' quality of life but might ultimately also lead to amputations and death (Brennan et al., 2017; Graves et al., 2022; Olsson et al., 2019). Despite impressive pre-clinical developments of wound dressings from novel biomaterials and nanotechnologies, the translation into commercially products has not been correlating impressive (Blanco-Fernandez et al., 2021). One hurdle to overcome this is to assure that promising products can be produced in a sustainable and green manufacturing setting.

Nanofibers, polymer mats with a nanometer-ranged fiber structure, have a certain promise when used as wound dressings (Thakkar and Misra, 2017; Uhljar and Ambrus, 2023; Grip et al., 2018). Nanofibers can fulfil many of the general demands of an ideal wound dressing, namely, 1) form a protective physical barrier helping avoiding infections, 2) create a wet environment with controlled humidity after swelling and removal of excess wound exudate, 3) allow gas and fluid exchange, and 4) provide thermic isolation, as well as 5) give an active support of the wound healing process. The active support of wound healing by nanofibers is postulated to be achieved by nanofibers mimicking the extracellular matrix (Frantz et al., 2010), and thus assist cell growth and proliferation. Active ingredients embedded in nanofibers are also excellently exposed to the wounded tissue, since

Abbreviations: CAM, Chloramphenicol; DAC, Dual asymmetric centrifugation; DMEM, Dulbecco's Modified Eagle's Medium; HPMC, Hydroxypropyl methylcellulose; *E. coli*, *Escherichia coli*; FBS, Fetal Bovine Serum; LipCAM, Chloramphenicol-loaded liposomes; LipRhodPE, Rhodamine labelled liposomes; LPS, Lipopolysaccharide; NO, Nitric oxide; PBS, Phosphate-buffered saline; PEO, Polyethylene oxide; PI, Polydispersity index; PVA, Poly (vinyl alcohol); RhodPE, Rhodamine-labelled lipids: 16:0 Liss Rhod PE 1,2-dipalmitoyl-*sn*-glycero-3-phosphoethanolamine-N-(lissamine rhodamine B sulfonyl) (ammonium salt); *S. aureus*, *Staphylococcus aureus*; SoyPC, Phosphatidylcholine from soybeans; VPG, Vesicular phospholipid gel; WES, Wire-electrospinning; ZP, Zeta potential.

* Corresponding author.
E-mail address: ann-mari.holsater@uit.no (A. Mari Holsæter).

https://doi.org/10.1016/j.ijpharm.2024.124136
Received 21 January 2024; Received in revised form 10 April 2024; Accepted 17 April 2024
Available online 19 April 2024

nanofibers provide a high surface-to-volume ratio. Finally, 6) biocompatible nanofibers can be formed since selecting non-toxic and also bioactive polymers from both synthetic and natural origin is highly viable (Juncos Bombin et al., 2020).

In electrospinning, polymer solutions transform into dry polymer fiber mates forming nanometer- ranged fiber structures. The most common and flexible electrospinning method for fabrication of nanofibers is needle-electrospinning. However, this technique has a poor fiber production rate and no commercial potential as such (Vass et al., 2020). The Nanospider™ NS Lab from Elmarco, used in this study, is a laboratory-sized wire-electrospinning (WES) machine that allows for an easy up-scaling (Elmarco, 2023). This technique allows multiple fibers to be formed from an electric charged wire when fed with a polymer solution under the influence of a strong electric field. Furthermore, the WES technology has several advantages over needle-electrospinning such as i) no clogging of the syringe with polymer solutions, ii) a high production speed, and iii) ease of setup and cleaning (Yalcinkaya, 2017).

Antimicrobial component(s) are often seen in wound dressings, since one of the leading causes of delayed wound healing are persistent infections (Sen, 2021). Successful antimicrobial therapy in wound healing means providing sufficient concentrations of the antimicrobial agent for a sufficient time. Having in mind that the need for frequent dressing changes is neither user-friendly nor optimal for the healing, a dressing that allows deposition of the antimicrobial agent in the wound for a longer time is desirable (Akombaetwa et al., 2023; Ingebrigtsen et al., 2017a).

We previously fabricated a wound dressing containing the antibiotic chloramphenicol (CAM) using WES (Schulte-Werning et al., 2021). In the current study, we targeted a more advanced formulation as compared to in the previous study, with liposomes as a secondary CAM-carrying nanostructure in nanofibers. Liposomes are well-known lipid-based nanostructures in nanomedicine, known to be highly biocompatible, formed from phospholipids as the main constituent. Conventional liposomes do not only have the potential to solubilize and stabilize drug molecules but have also been demonstrated to exhibit higher retention of entrapped drugs in the skin surface, and thus are promising carriers for dermal drug-delivery when targeting a depot-effect (Ternullo et al., 2017).

Accomplishing a sustained drug release from nanofibers as such is difficult and requires a careful selection of solvent, polymers, and drugs, often limiting the choice of polymers to be poorly water-soluble, which require the use of organic solvent and/or toxic acids during processing. This is not very environmentally friendly and demands ventilation and ideally also collection of the evaporated toxic solvent during processing. Alternatives, such as coaxial spinning and crosslinking of the electrospun nanofiber mats have also been tried for a more sustained release of drugs from nanofibers (Gaydhane et al., 2023). However, crosslinking of nanofibers for a more sustained drug release is often hampered by the demand of the use of toxic chemicals, whereas coaxial spinning to form "core–shell-nanofibers" is not feasible when using blend WES. Thus, we selected the "liposome-in-nanofiber formulation strategy" for obtaining a more sustained drug delivery and drug depot effect in wounds, while targeting a green production process and dressing through focusing on hydrophilic polymers that are permitting the use of water as the only solvent.

Although electrospinning of biopolymer-liposome hybrid systems has been reported before (Casula et al., 2023; Hasanbegloo et al., 2023; Mickova et al., 2012), the process remains challenging since the high electric current might damage the liposomes (Akombaetwa et al., 2023; Pires et al., 2019). To our knowledge "liposome-in-nanofibers" has not previously been produced by WES, which is a one-pot or blend technique where all ingredients are mixed in the same container. Therefore, extra care must be made not to apply solvents that destroy the liposomes, but at the same the spinning solution should have good spinning properties and be able to dissolve the fiber forming polymers. Thus, a mixture of aqueous liposome dispersion and aqueous polymer solutions is the preferred starting point in green, sustainable WES-nanofiber production making "liposome-in-nanofiber" formulations.

The aim of this study was to investigate the feasibility of preparing CAM-loaded-liposomes in nanofibers with green electrospinning using the WES technology. For this purpose, we chose water as an environmentally friendly, abundant solvent. The success of preparing the targeted and intact dual-nanostructured fiber dressings was confirmed by studying the fiber morphology in FE-SEM and with fluorescent-labelled liposomes in confocal microscope, in addition to assessing the drug release from the fiber dressings. Finally, the biological performance of the nanofibers was studied with respect to antimicrobial activity, anti-inflammatory activity as well as cytotoxicity *in vitro*.

2. Material and methods

2.1. Material

Lipoid S-100 (Soy-PC) (phosphatidylcholine ≥ 94 %) was a generous gift from Lipoid GmbH (Ludwigshafen, Germany). 16:0 Liss Rhod PE 1,2-dipalmitoyl-*sn*-glycero-3-phosphoethanolamine-N-(lissamine rhodamine B sulfonyl) (ammonium salt) (RhodPE) was produced by Avanti® Polar Lipids (Alabaster, Alabama, USA). Zirconium oxide beads (1.4 mm in diameter) were obtained from Bertin Technologies (Saint-Quentin-en-Yvelines, France). Methanol HiPerSolv CHROMANORM® HPLC grade and ethanol (96 % v/v) AnalaR NORMAPUR® were purchased from VWR International (Rosny-sous-Bois-cedex, France). Polyethylene oxide (PEO) (average Mw 900,000 g/mol) was produced by Dow Chemical Company (Midland, MI, USA). Cell-counting kit-8, chloramphenicol (CAM) (≥98 %), fetal bovine serum (FBS), lipopolysaccharides (LPS) (from Escherichia coli O55:B5), N-(1-Naphtyl)ethylenediamine dihydrochloride, pectin from citrus peel (85 % galacturonic acid, 78 % methoxy groups), penicillin–streptomycin, poly(vinyl alcohol) (PVA) (average Mw 85,000–124,000; 87–89 % hydrolysed), RPMI-1640 medium with L-glutamine and sodium bicarbonate, sulfanilamide and Tween® 80 were bought from Sigma-Aldrich (St. Louis, MO, USA). Hydroxypropylmethylcellulose (HPMC) (HPM, Benecel™ E4M HMC) was acquired from Ashland (Covington, KY, USA). Neonatal human dermal fibroblasts were obtained from Lonza Group AG (Basel, Switzerland). *Escherichia coli* (ATCC 25922), *Staphylococcus aureus* (ATCC 25923) and murine macrophages (RAW 264.7 cells) were acquired from ATCC (Manassas, VA, USA). Dulbecco's Modified Eagle Medium (DMEM) High Glucose was produced by Biowest (Nuaillé, France). Orthophosphoric acid ≥ 85 % was obtained from Kebo Lab Ab (Oslo, Norway). CAM Antimicrobial Susceptibility discs (30 µg, Oxoid™) were obtained from Thermo Fisher Scientific Inc. (Waltham, MA, USA).

2.2. Liposome preparation

CAM-containing liposomes (LipCAM) were prepared using the thin film hydration method, and by subsequent size-reduction by dual asymmetric centrifugation (DAC) as described previously (Holsæter et al., 2022). In brief, 200 mg of Soy-PC and 40 mg CAM were dissolved in methanol in a 20 ml brown injection vial. A lipid film was formed in the same injection vial by removal of the solvent by connecting the vial directly to a rotavapor (Büchi rotavapor R-124 with vacuum controller B-721, Büchi Vac® V-500, Büchi Labortechnik, Flawil, Switzerland) at 45 °C for approximately 1.5 h. For film hydration, 300 µl of distilled water and 500 mg of zirconium oxide beads (Ø = 1.4 mm) were added to the film before vortexing for 5 min. The lipid dispersion was stored overnight at 4 °C. The following day, the size of the liposomes was reduced, and the hydrated film was processed into a concentrated vesicular phospholipid gel (VPG) by homogenisation for 6 x 5 min at 3500 rpm using a DAC-machine, the SpeedMixer™ DAC 150.1 FVZ-K (Synergy Devices Ltd, High Wycombe, UK). The VPG was diluted with 1.5 ml distilled water to obtain a liposome dispersion after mixing for further 3

min at 3500 rpm in the DAC-machine, before removing the zirconium oxide beads by pipetting, and adjusting the volume to exactly 2 ml with distilled water, resulting in a final CAM- and Soy-PC concentration of 20 and 100 mg/ml, respectively.

Rhodamine-labelled liposomes (LipRhodPE) were prepared using thin film hydration method followed by size reduction by extrusion. 200 mg SoyPC and 2.0 mg of a rhodamine labelled phospholipid (RhodPE) were dissolved in methanol in a round bottom flask and a lipid film was formed as described above. The film was hydrated in 10 ml distilled water and stored in the fridge at 4 °C overnight before the liposome size was reduced by extrusion four times through a 400 nm pore size polycarbonate membrane (Nuclepore Track-Etch Membrane, Whatman House, Maidstone, UK).

2.3. Liposomal characterization

The liposomes size, size distribution (polydispersity index, PI) and zeta potential (ZP) were measured using the Zetasizer ZS Nano (Malvern, Oxford, UK). The liposome dispersions were diluted with filtered (0.2 μm) distilled water (LipCAM: 1:2000 (v/v), LipRhodPE: 1:200 (v/v)) and filtered (0.2 μm) tap water (LipCAM: 1:200 (v/v), LipRhodPE: 1:20 (v/v)), for size and zeta potential measurement, respectively. Two dilutions were prepared and measured from each batch; each measurement consisted of three machine runs. Three batches were prepared of LipCAM and one batch of LipRhodPE.

CAM entrapped in liposomes was calculated as given in Eq. 1, by quantifying CAM in the liposome dispersion before and after 4 h dialysis at room temperature in water (500 μl LipCAM, liposomes to water ratio: 1:500) using a dialysis bag with membrane (MwCO of 12–14 kD) (Spectra/Por™ 4 RC Dialysis Membrane Tubing, Spectrum Chemical Mfg. Corp., New Brunswick, NJ, USA). Before CAM quantification, the LipCAM were disrupted using methanol. The CAM content was measured by UV–Vis spectrophotometry using a Spark® reader (Tecan Trading AG, Männedorf, Switzerland) at $\lambda = 274$ nm. The entrapment efficiency was calculated using the following equation (Eq. 1):

Entrapment efficiency (%) = C_A/C_B x 100 %(1).

C_A: CAM content after dialysis.

C_B: CAM content before dialysis.

2.4. Preparation of polymer solutions for electrospinning

Five different polymer solutions were prepared with water as the only solvent. The different polymer solutions and their composition are listed in Table 1. The polymer solution (50 g in total) was stirred overnight at room temperature to ensure complete dissolution. For preparation of the PVA-solution, the mixture was heated up to 90 °C for approximately two hours to enable dissolution of the polymer at the given concentration.

Table 1
Total polymer concentration in the polymer solutions, and percentage (w/w) of each polymer present in the formulations.

Formulations	Polymer conc. (%)	Polymers (% of total) PEO	HPMC	Tween 80	Pectin	PVA
PEO	4.5	100	–	–	–	–
HPMC-PEO	4	50	50	–	–	–
HPMC-Tween 80-PEO	4	15	55	30	–	–
Pectin-PEO	4	50	–	–	50	–
PVA	10	–	–	–	–	100

Abbreviations: HPMC (hydroxypropylmethylcellulose), PEO (polyethylene oxide), PVA (poly (vinyl alcohol)).

2.5. Characterization of polymer solutions

The polymer solutions were characterized in terms of their surface tension, conductivity, and viscosity. Surface tension was measured with a K6 force tensiometer (Krüss GmbH, Hamburg, Germany) equipped with a Pt-Ir-ring K 610 (Krüss GmbH, Hamburg, Germany) using the Du Noüy ring method. A Sension™ + EC7 Basic Conductivity laboratory Kit (Hach, Loveland, CO, USA) was used to measure the conductivity. Both surface tension and conductivity were measured three times. The viscosity was measured using Haake™ Viscotester™ 7 plus (Thermo Electron GmbH, Karlsruhe, Germany) spindle TL7 at 22 ± 2 °C with the standard sample holder. The speed was set to 5 rpm, corresponding to a shear rate of 1.4 s^{-1}. The viscosity was recorded after one minute.

2.6. Preparation of polymer solutions with chloramphenicol and liposomes

Pectin and PEO solutions (Pectin-PEO) from Section 2.4 (Table 1) were prepared with CAM in the form of free CAM, LipCAM and free CAM combined with Soy-PC. The polymer solutions and the composition (% (w/w)) of the dry material are given in Fig. 1 and Table 2.

All solutions were made in water and the total dry weight kept at 4 % (w/w) (Fig. 1) with a CAM-concentration of 2 % (w/w) of the total dry content (Table 2). To obtain nanofibers containing free CAM and Soy-PC (Pectin-PEO-CAM-SoyPC), Soy-PC dissolved in ethanol was added to the CAM/pectin/PEO aqueous solution. The ethanol content in Pectin-PEO-CAM-SoyPC solution was kept at max 10 % (w/w) to avoid precipitation of pectin.

Nanofibers containing rhodamine labelled liposomes (Pectin-PEO-LipRhodPE) or free rhodamine lipids and Soy-PC (Pectin-PEO-RhodPE-SoyPC) were prepared as described above for Pectin-PEO-LipCAM and Pectin-PEO-CAM-SoyPC, except that 0.1 % RhodPE was replacing 2 % CAM. Contents are referred to as the percent of the dry material (Fig. 1 and Table 2). Each polymer solution and respective nanofiber was produced in triplicates.

2.7. Electrospinning of nanofibers

All nanofibers were electrospun applying the Nanospider NS Lab (Elmarco, Liberec, Czech Republik) as described previously (Schulte-Werning et al., 2021). A spinning voltage of 80 kV DC current was used. A one-sided carriage (40 ml) equipped with a metal orifice insert of 0.6 mm was filled with the polymer solution, and the polymer carriage speed was varied between 20 mm/s and 100 mm/s. The wire-to-collector-distance was kept at the maximum distance of 24 cm, and the substrate was stationary. The total spinning time was 80 (40 + 40) min for all solutions, with new polymer solution refilled after 40 min. Temperature and relative humidity were controlled to be at 25 ± 5 °C and 27 ± 7 %, respectively.

2.8. Nanofiber characterization

2.8.1. Field emission scanning Electron Microscopy (FE-SEM)

Morphology and diameter of the prepared nanofibers were determined by Field Emission Scanning Electron Microscopy (FE-SEM) using the Zeiss GeminiSEM 300 (Carl Zeiss Microscopy GmbH, Jena, Germany) microscope. All specimens were taken from the middle of the respective nanofibrous mats, mounted on the stubs using double-sided carbon tape and dried in a desiccator overnight. Prior to measurement, specimens were coated with gold/palladium by a Polacron SC7640 high-resolution sputter coater (Quorum Technologies LTD, Kent, UK). Three pictures were taken for each fiber mat. The software Image J (Rasband, 1997–2018) was used for fiber diameter determination by manually measuring the diameter of 100 fibers from the three separate pictures.

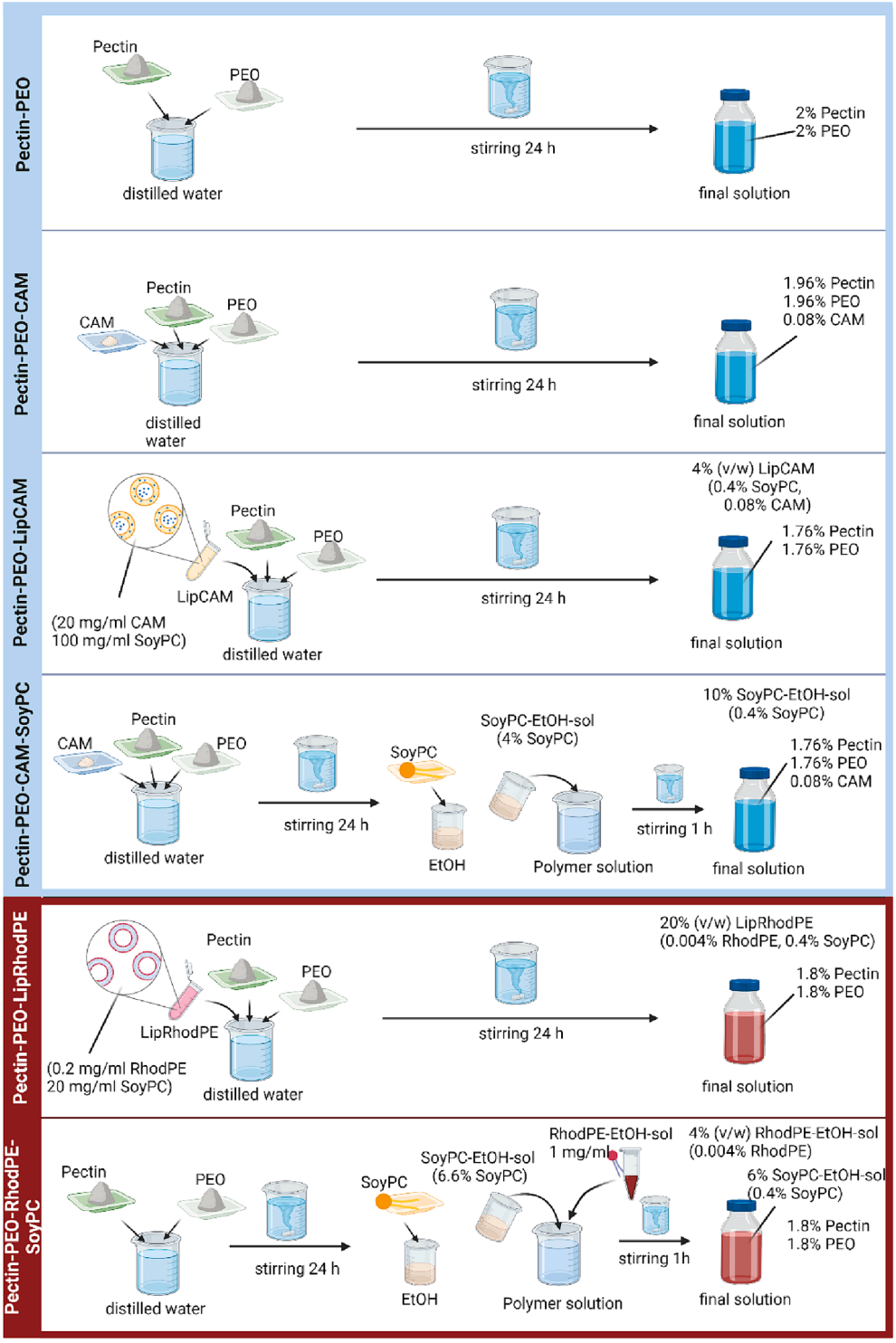

Fig. 1. Schematic illustration of the preparation procedure for making the polymer solutions with Chloramphenicol (blue) and RhodPE (red) either in liposomes or together with phospholipids (Soy-PC). If not indicated otherwise, all percentages are given as (w/w). Abbreviations: CAM (chloramphenicol), EtOH (ethanol), Lip (liposomes), LipCAM (chloramphenicol-loaded liposomes), LipRhodPE (rhodamine-labelled liposomes), PEO (polyethylene oxide), RhodPE (16:0 Liss Rhod PE (1,2-dipalmitoyl-*sn*-glycero-3-phosphoethanolamine-N-(lissamine rhodamine B sulfonyl))), sol (solution), SoyPC (phosphatidylcholine from soybeans). Created with BioRender.com.

2.8.2. Confocal imaging of rhodamine-nanofibers

Pectin-PEO-LipRhodPE and Pectin-PEO-RhodPE-SoyPC nanofibers were spun directly on 35 mm glass bottom microwell dishes (MatTek corporation, Ashland, MA, USA) for 10 s, using the same settings as applied before (Section 2.7). The confocal images were made by using a confocal laser scanning microscope: Zeiss LSM 880 (Carl Zeiss Microscopy GmbH, Jena, Germany) with the objective Plan-Apochromat 40x/1.2 and airyscan detection. Excitation of the rhodamine label (emission wavelength 583 nm) was done using the DPSS 651–10 laser. All images shown in this paper were adjusted applying gamma correction of 0.8 for optimal visualization using the software ZEN 2.3 (Carl Zeiss Microscopy GmbH, Jena, Germany), the same adjustments were

Table 2
Composition of dry material in the different pectin-PEO polymer solutions made to prepare nanofibers with different degree of complexity ranging from polymers only to chloramphenicol or RhodPE embedded in liposomes.

	Ingredients (w/w %)				
	Pectin	PEO	CAM	SoyPC	RhodPE
Pectin-PEO	50	50	–	–	–
Pectin-PEO-CAM	49	49	2	–	–
Pectin-PEO-LipCAM	44	44	2*	10*	–
Pectin-PEO-CAM-SoyPC	44	44	2	10	–
Pectin-PEO-LipRhodPE	45	45	–	10*	0.1*
Pectin-PEO-RhodPE-SoyPC	45	45	–	10	0.1

Abbreviations: CAM (chloramphenicol), Lip (Liposomes), LipCAM (chloramphenicol-loaded liposomes), LipRhodPE (rhodamine-labelled liposomes), RhodPE (16:0 Liss Rhod PE (1,2-dipalmitoyl-*sn*-glycero-3-phosphoethanolamine-N-(lissamine rhodamine B sulfonyl)), PEO (polyethylene oxide), SoyPC (phosphatidylcholine from soybeans).
* CAM and SoyPC, and RhodPE and SoyPC were added as LipCAM and LipRhodPE, respectively.

performed for all pictures.

For quantitative comparison, the grey values of the obtained confocal images (before gamma correction) were measured using the software Fiji (Schindelin et al., 2012). Briefly, a 3x3 raster was applied to the pictures and segmented lines were drawn on three fibers per raster, measuring the grey values as a measure of the intensity values of the fluorescence. The measurement was based on and modified from a method of Shihan et al. (Shihan et al., 2021). The obtained grey values were summarized in a histogram.

2.8.3. Texture and thickness of nanofibers

Tensile strength and elongation at break of the nanofiber mats were measured using a Texture Analyzer TA.XT plus (Stable Micro Systems Ltd., Surrey, UK) based on the ASTM-Standard D882-18 (ASTM International, 2018). Five specimens (10 x 80 mm) were cut from every fiber mat and the thickness was determined using an outside micrometer (0–25 mm, 0.001 mm, Wilson Wolpert Instruments, Aachen, Germany). The tensile strength and elongation at break for the nanofiber mats were determined by fastening the specimens between two tensile grips with an initial grip separation of 50 mm. The force needed to rupture the specimen was measured at a strain rate of 0.08 mm/s. The hereby obtained force-distance curve was automatically converted into a stress–-strain curve with the use of the specimen's dimensions. A toe compensation of the graph was performed and the tensile strength and elongation at break were determined using the Exponent connect Software v. 6.1.16.0 (Stable Micro Systems, Surrey, UK).

2.8.4. Fluid retention of nanofibers

Fiber specimen with a size of 2x2 cm were cut from the different nanofiber mats, weighed, and placed into weighing boats filled with 1 ml of simulated wound fluid (5.84 g/l NaCl, 3.60 g/l NaHCO3, 0.30 g/l KCl, 0.37 g/l CaCl2 x2H2O and 165 ml/l Albunorm®, modified after Bradford et al., 2009 (Bradford et al., 2009)). After 2 min, the excess fluid was removed from the weighing boats and the boats together with the remaining swollen fibers were weighed. The fibers were left to dry and the boat with the dried fibers were weighed to assess the loss of polymers during swelling.

Three specimens were tested per fiber mat and the fluid retention capacity and weight retained after drying was calculated as described in Eq. 2 and Eq. 3, respectively:

Fluid retention (%) = $(W_A\text{-}W_I)/W_I$ x 100 (2).

Weight retained after swelling (%) = W_L/W_I x 100 (3).

W_I: Initial weight of specimen.

W_A: Weight of specimen after swelling.

W_L: Weight of substance left on boat after test.

2.8.5. In vitro chloramphenicol release

The drug release of CAM containing nanofiber mats (Table 2) was assessed *in vitro* using jacketed Franz diffusion cells; 5 ml acceptor volume, 0.64 cm^2 donor diffusion area from PermeGear, Inc. (Hellertown, PA, USA). A cellophane membrane (Max Bringmann KG, Wendelstein, Germany) was placed in between donor and acceptor compartment, as described previously (Ingebrigtsen et al., 2017b). The acceptor medium, phosphate buffered saline (PBS) pH 7.4 (0.19 g/l KH_2PO_4, 2.98 g/l $Na_2HPO_4{\cdot}2H_2O$, 8 g/l NaCl), was kept at 32 °C. Round specimens with a diameter of 8 mm were cut from every fiber mat, weight and placed in the donor, where they were hydrated with 10 µl PBS. A solution of 100 µl CAM in PBS (2 mg/ml)) was used as control. After 15 and 30 min, and 1, 2, 4, 6, 8 and 24 h, a sample volume of 500 µl was taken and immediately replaced with fresh PBS. CAM was quantified with UV–Vis spectrophotometry at λ = 278 nm on a Spark® reader (Tecan Trading AG, Männedorf, Switzerland). Each sample batch was tested in duplicate.

2.9. Biological in vitro testing of nanofibers

2.9.1. Sample preparation for cell testing

For cell testing, samples were taken from the nanofiber mats and dissolved in Milli-Q-water to obtain a concentration of 10 mg/ml nanofibers. For lower concentrations, this solution was diluted 1:4 and 1:8 in cell medium.

2.9.2. In vitro cytotoxicity

The *in vitro* cytotoxicity of the nanofibers was tested in murine macrophages (RAW 264.7) and human dermal fibroblasts (NHDF-neo), using the Cell Counting Kit-8 (CCK-8, Sigma-Aldrich) cultured in complete RPMI medium, supplemented with 10 % (v/v) FBS and penicillin–streptomycin, or complete DMEM-hg, respectively. Cells were plated on 96-well plates (90 µl cell suspension/well; 1 x 10^5 cells/ml) followed by 24 h incubation at 37 °C, 5 % CO_2. Next, 10 µl of either medium (negative control) or samples were added to the cell suspension, resulting in fiber concentrations of 125, 250 and 1000 µg/ml. The plates were incubated for 24 h before 10 µl of CCK-8 reagent was added to each well, followed by another 4 h incubation. A Spark® multimode microplate reader (Tecan Trading AG, Männerdorf, Switzerland) was used, and absorbance measured at λ = 450 nm, with the reference wavelength set to λ = 650 nm. Cells treated in medium were the negative controls (100 % viability) (Schulte-Werning et al., 2021). All concentrations were tested in triplicates for each fiber batch.

2.9.3. Anti-inflammatory activity

Anti-inflammatory activity of the pectin-PEO nanofibers with and without active ingredient was tested using the same method as described previously (Schulte-Werning et al., 2021), measuring NO-production in LPS-stimulated murine macrophages (RAW 264.7). The cells were cultured in complete RPMI-medium, seeded on 24-well plates (1 ml/well, 5 x 10^5 cells/ml) and incubated for 24 h at 37 °C, 5 % CO_2. The RPMI-medium was removed and replaced with 900 µl LPS-containing medium (1 µg/ml). 100 µl of the dissolved nanofiber samples or medium as control, were added to each well, resulting in the same final fiber concentrations as tested in the cytotoxicity test (125, 250 and 1000 µg/ml). The cells were incubated for another 24 h. The cell supernatant was then removed, mixed with an equal amount of Griess reagent (0.1 % N-1-naphylenediamine dihydrochloride, 1 % sulfanilamide, 2.5 % phosphoric acid) and the absorbance measured on a Spark® multimode microplate reader (Tecan Trading AG, Männerdorf, Switzerland) at a λ = 540 nm. The relative NO-production of nanofiber treated cells was determined by comparing to non-treated, control cells (whose NO production was taken as 100 %). All concentrations were tested in triplicates for each fiber batch.

2.9.4. Antimicrobial activity

The antimicrobial activity of the nanofiber mats against *Escherichia*

coli (E. coli) and *Staphylococcus aureus (S. aureus)* was tested using a modified disc diffusion assay (Schulte-Werning et al., 2021). Bacterial suspensions in 0.9 % NaCl (adjusted to a turbidity of 0.5 McFarland) were spread evenly on Mueller-Hinton agar plates on an electric rotator using sterile cotton swabs. The samples (1.5 mg nanofiber mats, corresponding to 30 μg CAM; cut into Ø 6 mm discs) and the positive control (6 mm, 30 μg CAM disc, Thermo Fisher Scientific Inc. (Waltham, MA, USA)) were placed on the agar plates and incubated at 37 °C for 19 h. The diameters of the inhibition zones seen around the samples were measured using a scale. Each nanofiber was tested in three biological replicates.

2.10. Statistical analysis

To test for statistical significance, a one-way ANOVA followed by a Tukey test was performed using GraphPad Prism (Version 8.3.0, GraphPad Software, San Diego, CA, USA) and a p-value < 0.05 was considered statistically significant.

3. Results and discussion

Nanofibers versatility with respect to composition and ability to incorporate active ingredients, gives them a huge potential as (multi) functional wound dressings (Li et al., 2023; Schulte-Werning et al., 2021; Grip et al., 2018). The nanofibers are promising for achieving the desired drug release profiles, however, further research is needed to prove their industrial and therapeutic applicability (Kajdič et al., 2019). The development of nanofibers should therefore focus on general approaches, large-scale production, and new strategies for the development of sustainable therapeutic nanofibers.

This study focused on the use of liposomes as a second nano-sized vesicular drug carrier for CAM inside the nanofibers, aiming to achieve a sustained antimicrobial release from the nanofibers in treatment of infected wounds. First step was to investigate the spinnability of water-soluble polymers with WES (wire-electrospinning), since water is a safe solvent for later liposome incorporation, and since WES uses one polymer blend, feeding the wire. The processability of nanofibers and the formed fibers' mechanical- as well as morphological features, were also assessed for further processing of the same nanofibers with liposomes.

3.1. Selection of polymers for the nanofibers, spinning optimization and nanofiber characterization

For nanofiber to achieve their full potential as bioactive wound dressings, the applied polymers should be biocompatible, economically accessible, and be able to dissolve in an acceptable solvent with proper conductivity and viscosity that allow Taylors cones to form (Haider et al., 2018; Reneker and Yarin, 2008). Besides this, the selection of polymers for this study was based on their expected spinnability and solubility in water as a single solvent, as well as the polymers biocompatibility and swelling abilities, leading to the selection of four polymers: PEO, HPMC, Pectin and PVA for our five prepared formulations (Table 1).

PEO is a non-toxic, hydrophilic and synthetic polymer, widely used in electrospinning as co-polymer to support the formation of nanofibers (Grip et al., 2018; Schulte-Werning et al., 2021; Stie et al., 2019), but PEO might also be spun as the sole polymer, and has the ability to form nanofibers when electrospun from aqueous solution (Filip and Peer, 2019; Ramakrishnan et al., 2019). However, in this set-up we experienced that the PEO-solutions had a very slow formation of Taylors cone, which is reflected by the selected carriage speed of only 20 mm/s (Table 3). The slower formation of Taylor cones relative to the other polymer solutions could not be related to the applied electrical voltage, temperature or humidity, since these process- and ambient parameters were kept the same for all polymer solutions (Section 2.7). The final polymer concentration of 4.5 % for PEO is in the same concentration range as the other solutions, except for PVA, where a final polymer concentration of 10 % (w/w) was applied. The concentration is highly relevant, since the formation of nanofibers in electrospinning emerges as the stretching of the charged jets happens (Pillay et al., 2013; Reneker and Yarin, 2008). Thus, the chain entanglement between polymeric chains in this jet improves with increased concentration, whereas a low polymer concentration will result in jet fragmentation (spraying) due to lack of needed contact between polymers. Also, a too high concentration might cause problems with regards to viscosity and surface tension, as this will disrupt the flow of the solutions needed to feed the wire during spinning. Wire electrode is a design using a fixed wire stringed over the spinning area. The carriage containing with the polymer solution move along the wire electrode, coating it with the solution. As it can be seen in Table 3, the PEO-solution had the second highest viscosity of all solutions, which means that increasing the polymer concentration to improve the processability was not an option. Probably, it is the low conductivity of the PEO-solution that hindered the formation of Taylors cone and efficient fiber formation. This is supported by the fact that the surface tension is approximately the same for all solutions (Table 3), but PEO had a very different and lower conductivity compared to the other solutions. The conductivity could have been changed by adding salt or a cosolvent, as demonstrated earlier (Ramakrishnan et al., 2019), but in this case further optimization was not conducted.

Table 3
Characterization and electrospinning settings of solutions with different hydrophilic polymer systems (Results are presented as mean ± SD).

	PEO	HPMC-PEO	HPMC-Tween 80-PEO	Pectin-PEO	PVA
Surface tension (mN/m)	59 ± 0.6	50 ± 1.2	45 ± 1.3	59 ± 0.3	47 ± 0.6
Conductivity (μS/cm)	64 ± 1.7	212 ± 0.6	198 ± 0.5	1286 ± 12.7	788 ± 0.6
Viscosity (mPas)	5730	6320	1910	1460	830
Carriage speed (mm/s)	20	30	30	100	50

Abbreviations: PEO (polyethylene oxide), HPMC (hydroxypropylmethylcellulose), PVA (poly (vinyl alcohol)).

HPMC is hydrophilic cellulose derivative with good swelling ability, and thus helpful in obtaining a more controlled drug release (Mašková et al., 2020). It is extensively studied as copolymer in electrospinning and already showed promising results for use in nanofibrous wound dressings by our group (Grip et al., 2018; Schulte-Werning et al., 2021). HPMC was not spun alone since it has been demonstrated that HPMC used as a single polymer tends to form heterogeneous fibers with beads on their surface (Aydogdu et al., 2018). Thus, adding PEO or other ingredients that help lowering the tension between HPMC-polymer chains by impacting the formation of hydrogen bonds with HPMC is advisable (Filip and Peer, 2019; Olechno et al., 2022). To add also Tween-80 to this PEO-HMPC polymer blend was inspired by Aydogdu et al., (Aydogdu et al., 2018) who found that a HPMC, Tween 80 and PEO-mixture when spun in water as single solvent formed bead-free nanofibers when using the traditional needle-electrospinning. Both the HPMC-containing polymer blends showed an improved fiber formation compared to PEO alone, but again the productivity was not optimal, as reflected by the low carriage speed, and explained by the relatively low conductivity, as compared to the last two polymers formulations investigated: Pectin-PEO and PVA.

Pectin is a biocompatible and biodegradable natural polysaccharide found in the cell wall and intercellular region of higher plants, and it is usually obtained from citrus or apple peels (Li et al., 2021). Pectin mainly consists of (1 → 4)-α-D-galacturonic acid units, making it both biodegradable and biocompatible (Mohnen, 2008). Like to HPMC, to pectin is usually added a co-polymer like PEO or PVA to improve chain entanglement (Rockwell et al., 2014; Xu et al., 2022). Of particular

interest for this project was the known ability of pectin to stabilize liposomes (Smistad et al., 2012), together with its low toxicity and high gelling abilities (Han et al., 2022).

PVA is a biocompatible and biodegradable hydrophilic polymer, with a wide application in medicine. We selected medical grade PVA with an average Mw 85,000–124,000; 87–89 % hydrolyzed, allowing a higher polymer concentration than the other applied polymer solutions tested in the study. We successfully electrospun nanofibers from a 10 % (w/w) solution, which still gave the lowest viscosity of all solutions (Table 3). This concentration however corresponded well to what has been described in similar formulations demonstrating PVA spinning abilities when dissolved in water (Park et al., 2010).

In wire electrospinning, when voltage is applied to the wire, many Taylor cones form along the wire and fibers are ejected, travelling up to the collector electrode above the wire. In our previous work, where we used solutions containing ethanol, we observed very fast fiber formation and could use the maximum carriage speed (300 mm/s) (Grip et al., 2018; Schulte-Werning et al., 2021). All carriage speeds in this study were lower (between 20 and 100 mm/s) compared to the carriage speed used in our previous studies (300 mm/s) (Grip et al., 2018; Schulte-Werning et al., 2021). However, carriage speeds in a similar range as in this study have been reported in other studies: Fareed at al (Fareed et al., 2022) used a carriage speed of 90 mm/s for gum Arabic/PVA nanofibers and Ramakrishnan et al (Ramakrishnan et al., 2019) had a carriage speed of 100 mms/s for PEO nanofibers with NaCl. Since the electric field between the electrodes needs to be strong enough to overcome the surface tension to form fibers (Yalcinkaya, 2017), the lower carriage speed was probably due to a higher surface tension of the water-based solutions. In this study, a surface tension of 45–60 mN/m was observed (Table 3), whereas in previous solutions with ethanol the surface tension was only 26–28 mN/m (Schulte-Werning et al., 2021). In the current study, the solution containing the surfactant Tween 80 had the lowest surface tension (45 mN/m), however still higher than the surface tension of ethanol containing solutions, which is also reflected by the poorer productivity compared to what was observed earlier.

Conductivity seems, however, to be the most critical factor controlling the speed of fiber formation, as the fiber formation rate of the solutions can be ranked according to their conductivity (Table 3). Pectin-PEO showed the highest fiber formation rate (100 mm/s) and the highest conductivity (1286 μS/cm), which was expected because of the anionic (1 → 4)-α-D-galacturonic acid units that are dominating the structure of pectin. The important role of the conductivity on fiber formation is well known; it is one of the main factors influencing the Taylor cone formation. Taylor cone formation is depending on the availability of free charges that can move to the polymer solution's surface when an electric field is applied, thus forming the Taylor cone. If the conductivity is too low, no fiber formation will occur (Angammana and Jayaram, 2011; Haider et al., 2018).

All solutions were spun for a fixed time of 40 + 40 min and the fiber mat thickness and its weight per area was measured to determine the fiber formation rate (Table 4). The successful nanofiber formation was also determined by observing the level of defect-free nanofibers in SEM and measurement of the fiber diameter (Fig. 2).

Table 4
Thickness and density of nanofibers spun from the different polymer solutions (n = 5). Results are presented as mean ± SD.

	PEO*	HPMC-PEO	HPMC-PEO-Tween 80	Pectin-PEO	PVA
Mat thickness (μm)	–	23 ± 4.8	18 ± 1.8	27 ± 2.6	30 ± 1.1
Mat weight per cm^2 (mg)	–	0.6 ± 0.14	0.5 ± 0.09	1.5 ± 0.35	0.6 ± 0.12

* PEO-nanofibers could not to be removed from the substrate and were therefore not assessed. Abbreviations: PEO (polyethylene oxide), HPMC (hydroxypropylmethylcellulose), PVA (poly (vinyl alcohol)).

PEO-solution had a very slow fiber formation, and no coherent mat was therefore formed during the 80 min spinning time. In addition, wet areas remained on the mat after spinning, making it impossible to lift off the fibers from the substrate. All other polymers formed coherent fiber mats that could be lifted from the substrate and used in further analyses. PVA nanofiber mat had the highest thickness of 30 μm, but the Pectin-PEO mat had the highest mat weight per area with 1.5 mg/cm^2 (Table 4). In general, the mat thickness and the mat weight per area were higher with a higher carriage speed, which was as expected.

To confirm that nanofibers were formed and to investigate their morphology and fiber diameter, which might influence not only their mechanical properties, but also cell attachment (Kim et al., 2016), SEM pictures were prepared from all the different formulations (Fig. 2). These pictures showed that all polymer systems produced bead-free fibers, but with varying mean diameters. Fibers consisting of PVA had the largest mean fiber diameter with 182 nm, and Pectin-PEO fibers the lowest diameter, with a mean diameter of 53 nm. This might explain that Pectin-PEO fibers had a lower mat thickness but a higher mat weight per cm^2 than the PVA fibers: because of the smaller fiber diameter, the Pectin-PEO mat probably has a higher fiber density then the PVA mat. The fiber distribution for HPMC-Tween 80-PEO-fibers is similar to that of HPMC-PEO fibers but shifted towards lower diameter values. This finding is most likely due to the introduction of Tween 80 to the solution that lowered the surface tension but at the same time led to a reduction of the concentration of the HPMC and PEO in the solution, which reduced the viscosity (Table 3). The same correlation between polymer concentration, viscosity and fiber diameter of HPMC-PEO-fibers has been reported before (Aydogdu et al., 2018).

A fibrous dressing should have sufficient mechanical strength to allow normal handling by the user, as well as during manufacturing, packing and transport. Thus, the tensile strength and elongation of break of all nanofibers that had formed a removable fiber mat were tested. Since the PEO-nanofibers did not have sufficient mechanical strength to be loosened from the substrate, they were not included in this examination (Fig. 3). The tensile strength (Fig. 3A) refers to the force needed to rupture the fiber mat, while the elongation at break (Fig. 3B) shows the ductility of the material. Pectin-PEO fibers had the highest tensile strength, around three times higher than that of the other fibers. In contrast, PVA fibers showed the highest elongation at break. Kim et al., found a general trend that an increase in fiber diameter led to lower tensile strength and higher elongation at break and vice versa for PCL-nanofibers (Kim et al., 2016). In our study we could observe the same tendency, especially for the small diameter Pectin-PEO fibers and the large diameter PVA fibers, although these contained different polymers. We decided to prioritize the tensile strength for the ease to handle over stretching qualities, hence moving forward with the Pectin-PEO fiber mat as formulation of choice for a high tensile strength.

The nanofibers in this study are intended for the use as wound dressings in chronic wounds, where the production of varying amounts of exudate often presents a challenge. Thus, the dressing should absorb the exudate, provide a moist wound healing environment, and avoid exudate leakage to prevent wound infection (Hasan et al., 2023). We regarded it desirable to select the nanofiber with the highest absorption capacity and measured the retention of simulated wound fluid in the fibers (swelling index) as well as the weight of the fibers in dry state after the test (weight retained after test), to see potential polymer loss of the fibers (Fig. 4). Interestingly, we observed that the Pectin-PEO mat stayed mostly intact for the two minutes, turning into a sticky gel upon removal of excess fluid, while the other fibers, especially HPMC-Tween-80-PEO and PVA fibers disintegrated and did not form a coherent swollen fiber mat when the excess fluid was removed. This observation is supported by the lower weight retention after the test (Fig. 4B). Low weight retention can probably be explained by parts of the polymers being dissolved and thereafter removed together with the excess fluid. This also explains the corresponding lower swelling index of HPMC-PEO, HPMC-Tween 80-PEO and PVA fibers.

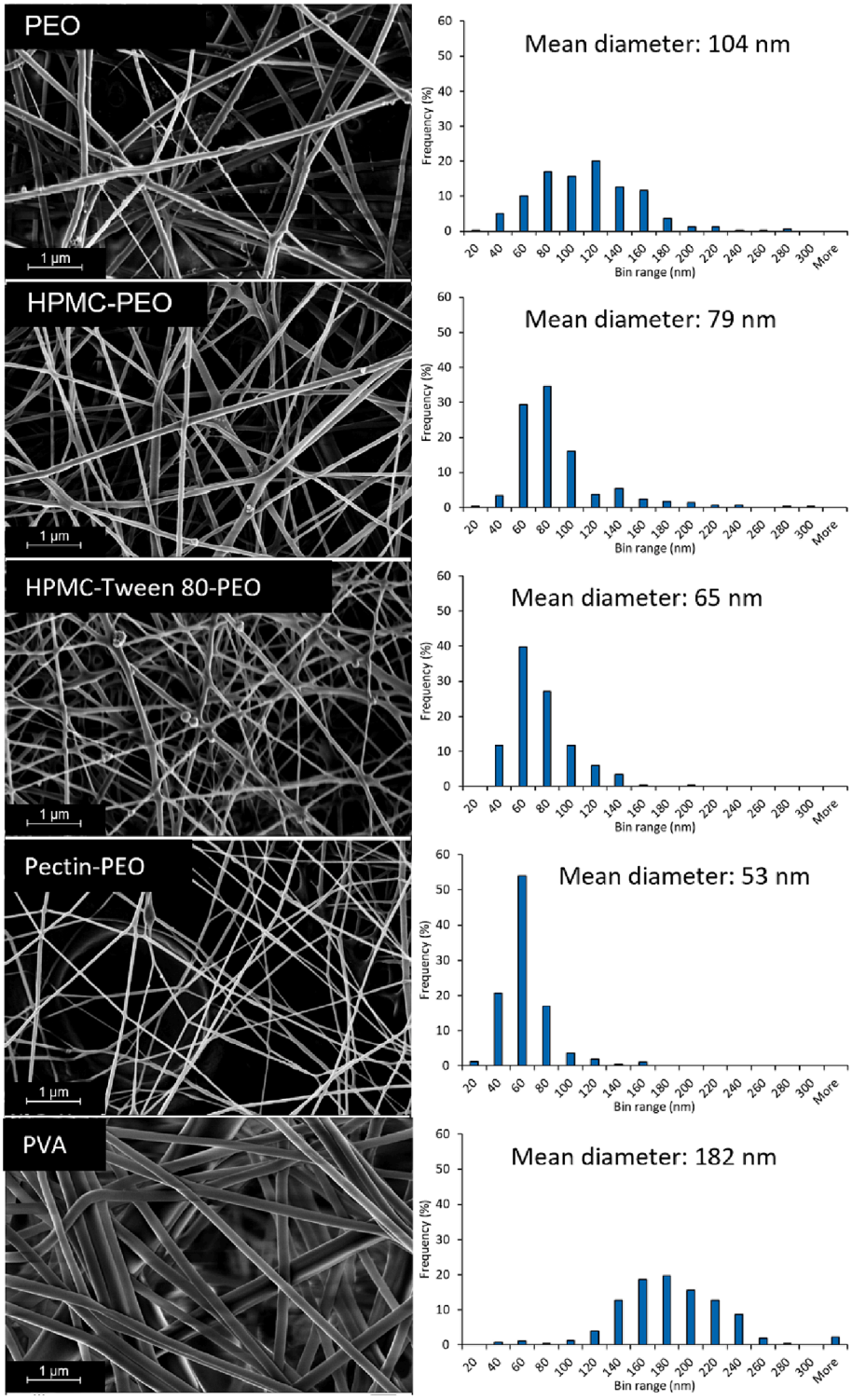

Fig. 2. Nanofiber morphology observed by SEM. The mean diameter and diameter distribution were determined by Image J software, measuring the diameter of 100 fibers per image. Abbreviations: HPMC (hydroxypropylmethylcellulose), PEO (polyethylene oxide), PVA (poly (vinyl alcohol)).

The gel- forming ability of the Pectin-PEO fibers is demonstrated by the highest swelling index, and the highest weight retention after the test. This finding is supported by Kowalski et al., who examined the swelling of pectin-based hydrogels and found that the addition of pectin to other hydrogels could increase their swelling ratio (Kowalski et al., 2019). The observed weight retention higher than 100 % is most likely due to retention of the salts from the simulated wound fluid in the fibers after drying.

Because of the high fiber formation rate, high tensile strength, and high swelling ability, Pectin-PEO nanofibers were selected for further studies, including active ingredient (CAM) and liposomes for controlled or sustained delivery of the active ingredient to the wound. This solution allowed for the highest carriage speed with only water as solvent, yielding fibers with a high mat thickness and a high weight per area, all favorable characteristics for a potential scale-up.

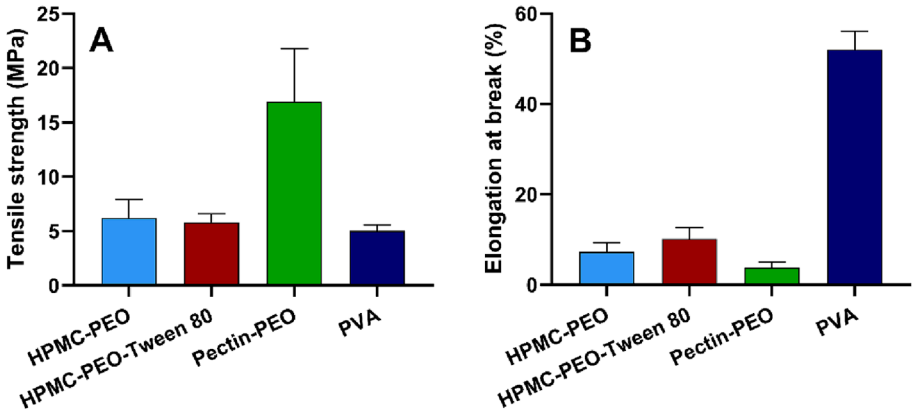

Fig. 3. Tensile strength (A) and elongation at break (B) as a measure for the mechanical properties of the successfully formed nanofibers. Five specimens were cut and examined from each formulation. Results are presented as mean ± SD (n = 5). Abbreviations: HPMC (hydroxypropylmethylcellulose), PEO (polyethylene oxide), PVA (poly (vinyl alcohol)).

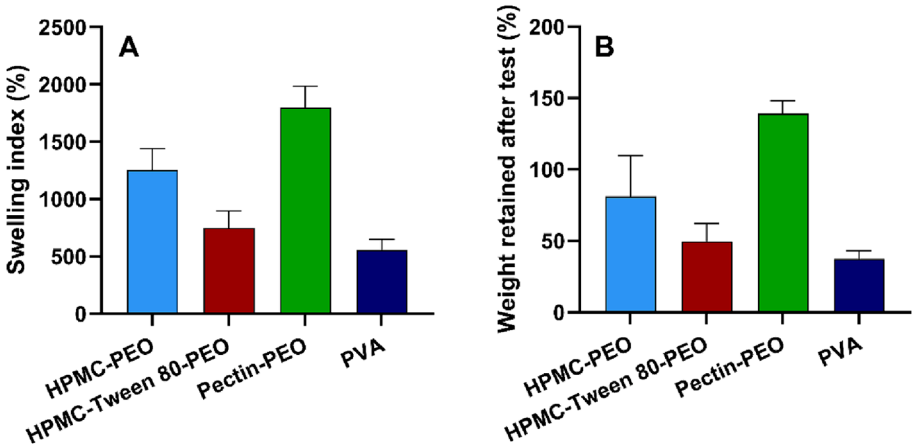

Fig. 4. Nanofibers swelling index (A) after 2 min exposure to artificial wound exudate, and weight retained (B) after drying. Results are presented as mean ± SD (n = 3). Abbreviations: HPMC (hydroxypropylmethylcellulose), PEO (polyethylene oxide), PVA (poly (vinyl alcohol)).

3.2. Liposomes characterization

When liposomes are incorporated into nanofibers, they might affect the spinning behavior of the polymer solution. Gómez-Mascaraque et al. reported that big-sized liposomes disturbed the Taylor cone during electrospraying and led to dripping of the solution, while liposomes of a size between 200 to 770 nm could be sprayed successfully (Gómez-Mascaraque et al., 2017). Based on this and the finding of Verma et al., who showed that liposomes with a size 272 nm delivered their load into stratum corneum and slightly into viable dermis and dermis (Verma et al., 2003), we aimed to fabricate liposomes with a size under 300 nm. In addition, since intact liposomes should be present in the nanofibers after electrospinning, not only liposomes with CAM, but also similar liposomes with fluorescent rhodamine labelled lipids (RhodPE) were prepared for easier examination in confocal microscopy. Liposomal size, polydispersity index, zeta potential and CAM-entrapment efficiency are shown in Table 5. As planned, LipRhodPE had a similar size as LipCAM (Table 5). The zeta potential of LipCAM was close to neutral while the surface charge of LipRhodPE had a negative zeta potential (ZP), probably due to the presence of the labelled head group. LipCAM had a drug entrapment efficiency (EE) of 55 %, similar to that reported previously for CAM-loaded liposomes made of Soy-PC (Ingebrigtsen et al., 2017a).

Table 5
Liposome characterization of CAM-containing liposomes (LipCAM) and rhodamine-labelled liposomes (LipRhodPE). Results are presented as mean ± SD (n = 3 for LipCAM and n = 1 for LipRhodPE).

	Liposome diameter (nm)	PI	Zeta potential (mV)	Entrapment efficiency (%)
LipCAM	275 ± 40	0.20 ± 0.02	− 6.7 ± 2.9	55 ± 9
LipRhodPE	289	0.21	− 27.3	–

Abbreviations: CAM (chloramphenicol), LipCAM (chloramphenicol-loaded liposomes), LipRhodPE (rhodamine-labelled liposomes), PI (Polydispersity index).

3.3. Electrospinning and characterization of pectin-PEO-nanofibers loaded with chloramphenicol-liposomes

For reducing the infection burden in chronic wounds, we chose to add CAM to the dressing. To address the common issue of undesired burst release in blend electrospinning (Homaeigohar and Boccaccini, 2020), especially when hydrophilic polymers are used (Schulte-Werning et al., 2021), and achieve a more sustained release, we incorporated our drug CAM into liposomes (LipCAM) before nanofiber fabrication (Pectin-PEO-LipCAM).

To assess the effect of this liposomal formulation within the nanofibers we included two controls: i) free CAM in nanofibers (Pectin-PEO-

CAM) and ii) free CAM and free phosphatidylcholine from soybeans (Soy-PC) in nanofibers – as a physical dispersion not arranged in liposomes (Pectin-PEO-CAM-SoyPC).

3.3.1. Morphological characterization

Nanofiber morphology and diameter are important parameters of nanofibers, affecting their function and behavior and are also indicators of nanofiber quality and the electrospinning process. Polymer concentration, solution characteristics, spinning settings as well as temperature and humidity influence the electrospinning process and hence fiber morphology and diameter (Haider et al., 2018). To see whether the incorporated active ingredient and the liposomes had an influence on the electrospinning process and therefore nanofiber morphology, we compared the SEM-images and diameter distributions of Pectin-PEO nanofibers with SEM-images of the nanofibers with the active ingredients (Fig. 5).

All solutions formed randomly oriented nanofibers without visible artefacts. The mean fiber diameter of all fibers ranged between 60 and 70 nm, little variation in the diameter between the different fibers was observed. The formation of defect-free nanofibers with a mean diameter in a narrow range amongst all solutions, even from solutions containing CAM, LipCAM or CAM-SoyPC, suggests that the pectin-PEO polymer system is a robust system suitable for electrospinning of the active ingredients and that the addition of the active ingredients resulted in successful electrospinning. Furthermore, the defect-free morphology visible in the SEM-pictures and the small batch to batch variations in diameter visible in the histograms, confirm the use of suitable electrospinning settings for reproducible fiber formation.

Yu et al., suspected that phase separation occurred during electrospinning of phosphatidylcholine (PC)-PVP nanofibers from electrospinning solutions containing 10 % (w/w) PC, visible as PC-nanoparticles on the fiber surface (Yu et al., 2011). No impurities can

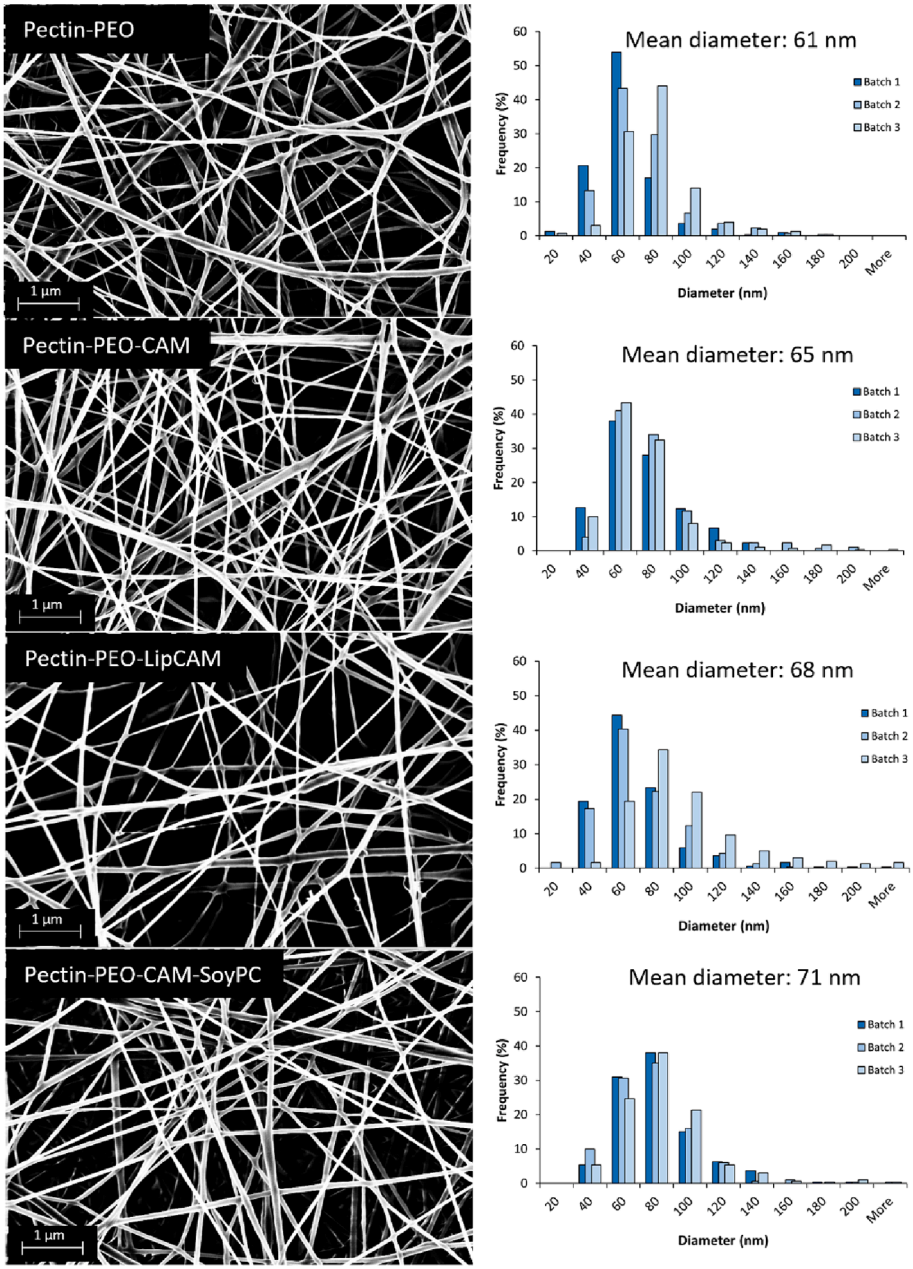

Fig. 5. Morphology seen by SEM imaging, mean diameter and diameter distribution determined by Image J software. Abbreviations: CAM (chloramphenicol), LipCAM (chloramphenicol-loaded liposomes), PEO (polyethylene oxide), SoyPC (phosphatidylcholine from soybeans).

be seen on the surface of Pectin-PEO-LipCAM or Pectin-PEO-CAM-SoyPC in this study, suggesting that the PC concentration used in this study (10 % SoyPC in the dry material (Table 2)) did not lead to phase separation and that the liposomes, if they stayed intact, did remain within the nanofibers and did not aggregate on the surface of the nanofibers.

Having in mind that the high shear force working on the polymer jet during electrospinning, might damage the liposomal membrane, especially in blend electrospinning (Mickova et al., 2012), we electrospun LipRhodPE of the same size and similar properties as LipCAM into nanofibers (Pectin-PEO-LipRhodPE). This allowed us to evaluate the intactness of the liposomes in the nanofibers after spinning.

As control we used an electrospinning solution that contained free RhodPE together with free Soy-PC. Both lipids were dissolved in ethanol before it was added to the Pectin-PEO-solution (Pectin-PEO-RhodPE-SoyPC) (Fig. 1). Representative confocal images of Pectin-PEO-LipRhodPE and Pectin-PEO-RhodpE-SoyPC can be seen in Fig. 6A and 6B, respectively. The fluorescence signals visible in both pictures follow a fibrous pattern, similar to that visible in SEM-pictures of Pectin-PEO-LipCAM and Pectin-PEO-CAM-SoyPC (Fig. 5). Pectin-PEO-LipRhodPE showed a non-uniformly distributed fluorescence pattern inside the nanofibers with punctuated high-fluorescent regions. This pattern indicates the presence of intact liposomes, with the high-intensity fluorescence regions coming from intact LipRhodPE (Fig. 6A). A more uniform distribution of the rhodamine-labelled lipids would be expected if the liposomes broke during electrospinning, as was the case for the control, Pectin-PEO-RhodPE-SoyPC (Fig. 6B). This finding is supported by similar fluorescence patterns that have been observed when rhodamine-labelled liposomes were spun into nanofibers and stayed intact (Chandrawati et al., 2017; Li et al., 2014). The fluorescence signals associated with the liposomes seem very elongated. The mean diameter of the nanofibers of 68 nm, although somewhat wider than the nanofibers without liposomes (61 nm) (Fig. 5), is narrow taking into account the mean diameter of liposomes, of 275 ± 40 (Table 5). Thus, the liposomes were most likely stretched during the electrospinning process due to jet stretching. The same effect has been observed by Li et al., who spun SUVs in PVP and sodium hyaluronate core–shell nanofibers and saw elliptical SUVs in TEM-pictures in the nanofiber core (Li et al., 2014). Looking at confocal pictures of Pectin-PEO-Rhod-SoyPC, certain areas show a scattered fluorescence pattern similar to that of Pectin-PEO-LipRhodPE, however the total fluorescence distribution looks more uniform than that of Pectin-PEO-LipRhodPE.

To obtain a quantitative comparison between the liposome versus lipid-dispersion containing formulations, we measured the grey values in the visible nanofiber structures and plotted the data (Fig. 7). The maximum, minimum and median grey value measured for each formulation are summarized in Table 6. These values confirmed that Pectin-PEO-LipRhodPE has a higher number of high grey values compared to Pectin-PEO-RhodPE-SoyPC, visible in higher maximum, mean and median grey values. It is visible that the grey values of Pectin-PEO-RhodPE-SoyPC are distributed more in the lower value ranges while the grey values of Pectin-PEO-LipRhodPE are shifted towards

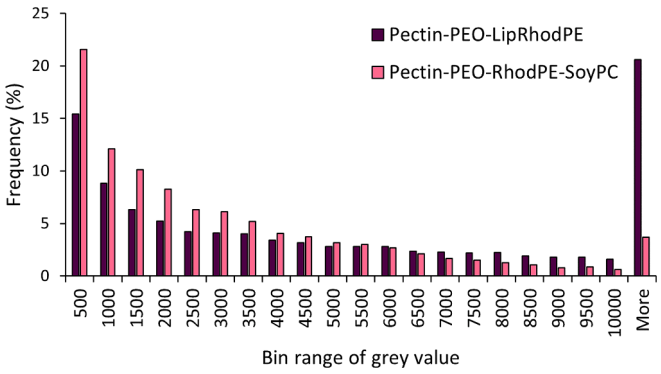

Fig. 7. Frequency distribution of grey values measured across confocal images of nanofibers containing rhodamine-labelled liposomes (Pectin-PEO-LipRhodPE) and nanofibers containing rhodamine-labelled lipids together with phosphatidylcholine from soybeans (Pectin-PEO-RhodPE-SoyPC). Abbreviations: LipRhodPE (rhodamine-labelled liposomes), PEO (polyethylene oxide), RhodPE (16:0 Liss Rhod PE (1,2-dipalmitoyl-*sn*-glycero-3-phosphoethanolamine-N-(lissamine rhodamine B sulfonyl))), SoyPC (phosphatidylcholine from soybeans).

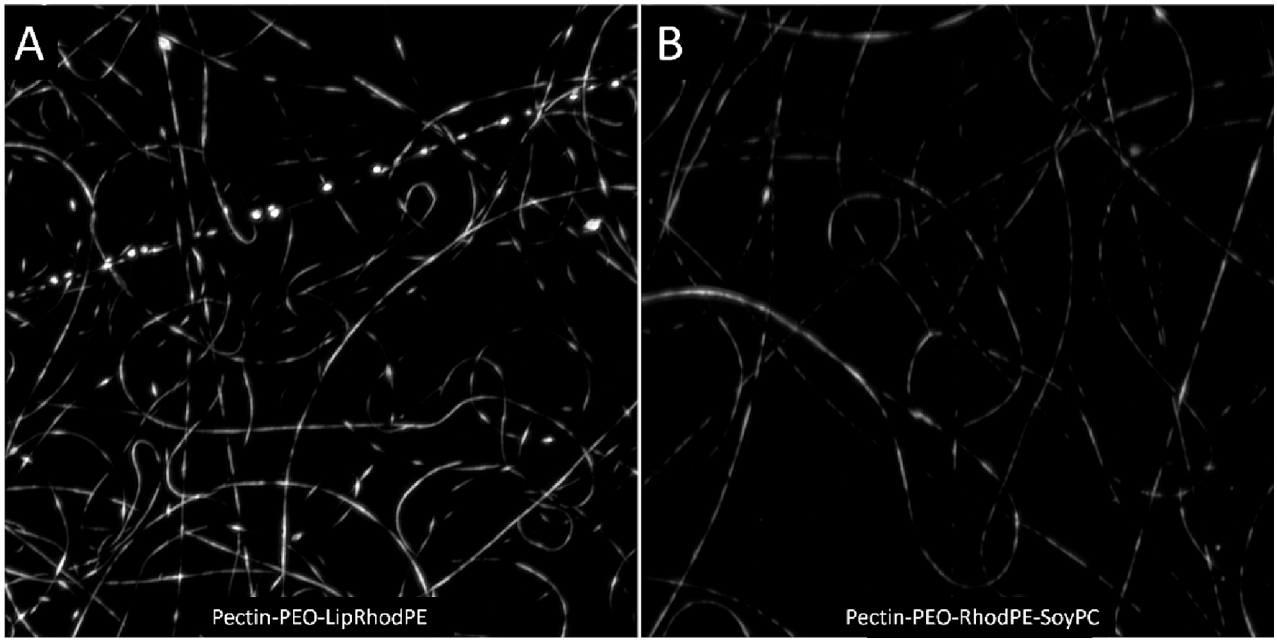

Fig. 6. Confocal images of nanofibers containing rhodamine-labelled liposomes (Pectin-PEO-LipRhodPE) (A) and nanofibers containing rhodamine-labelled lipids together with phosphatidylcholine from soybeans (Pectin-PEO-Rhod-SoyPC) (B). Abbreviations: LipRhodPE (rhodamine-labelled liposomes), PEO (polyethylene oxide), RhodPE (16:0 Liss Rhod PE (1,2-dipalmitoyl-*sn*-glycero-3-phosphoethanolamine-N-(lissamine rhodamine B sulfonyl))), SoyPC (phosphatidylcholine from soybeans).

Table 6
Maximum, mean and median grey value measured in confocal images of nanofibers containing rhodamine-labelled liposomes (Pectin-PEO-LipRhodPE) and nanofibers containing dispersed rhodamine-labelled lipids together with phosphatidylcholine from soybeans (Pectin-PEO-RhodPE-SoyPC).

	Maximum grey value	Mean grey value	Median grey value
Pectin-PEO-LipRhodPE	46,393	6063	3784
Pectin-PEO-RhodPE-SoyPC	22,702	2879	1874

Abbreviations: LipRhodPE (rhodamine-labelled liposomes), PEO (polyethylene oxide), RhodPE (16:0 Liss Rhod PE (1,2-dipalmitoyl-*sn*-glycero-3-phosphoethanolamine-N-(lissamine rhodamine B sulfonyl))), SoyPC (phosphatidylcholine from soybeans).

higher value ranges. This quantitative data supports the impression obtained from the pictures: Pectin-PEO-LipRhodPE have a higher punctual intensity compared to Pectin-PEO-RhodPE-SoyPC, which supports the presence of intact liposomes in the nanofibers.

3.3.2. Mechanical characterization

The thickness, mat weight per area and mechanical properties of the pectin-PEO fibers with incorporated active ingredients were tested to investigate how the mechanical properties were maintained when lipids and CAM were added (Table 7, Fig. 8). Since adding active ingredients and liposomes can affect nanofiber's mechanical properties (Lanno et al., 2020; Cui et al., 2018; Ge et al., 2019), we made a full comparison of all four nanofibers. The addition of free CAM into the Pectin-PEO nanofibers did not significantly change their tensile strength or elongation at break compared to that of pure Pectin-PEO fibers. However, although the SEM-pictures of Pectin-PEO-CAM, Pectin-PEO-LipCAM and Pectin-PEO-CAM-SoyPC did not show any defects or change in fiber diameter compared to Pectin-PEO fibers (Fig. 5), Pectin-PEO-LipCAM and Pectin-PEO-CAM-SoyPC had a significant lower tensile strength compared to Pectin-PEO fibers (Fig. 8A). This finding is similar to the findings of Ge et al. (Ge et al., 2019).

Pectin-PEO-CAM contains 2 % CAM, while Pectin-PEO-LipCAM and Pectin-PEO-CAM-SoyPC contain 2 % CAM and 10 % Soy-PC (Table 2). With the presence of lipids, the total polymer content was decreased. This might have weakened the polymer network leading to the reduction in tensile strength. In addition, although the nanofibers thickness remained the same after addition of the active ingredients (Table 7), the mat weight per area was reduced for Pectin-PEO-LipCAM and Pectin-PEO-CAM-SoyPC, indicating a lower fiber network density, which could also reduce the tensile strength.

Although the incorporation of LipCAM and CAM-SoyPC into Pectin-PEO-nanofibers decrease the tensile strength, this did not hinder the dressings from enduring normal handling. The overall tensile strength of these formulations is still within the range reported for pectin-PEO-nanofibers: Cui et al. reported a tensile strength of 14.6 ± 5.2 MPa for pectin-PEO-nanofibers from citrus peel pectin and Rockwell et al., found a tensile strength around 4.5 MPa for pectin-PEO-nanofibers (Cui et al., 2016; Rockwell et al., 2014).

Table 7
Thickness and mat weight per area of nanofibers. Results are presented as mean with their respective SD (n = 3).

	Pectin-PEO	Pectin-PEO-CAM	Pectin-PEO-LipCAM	Pectin-PEO-CAM-SoyPC
Mat thickness (μm)	28.5 ± 2.0	26.2 ± 3.5	31.4 ± 3.9	27.3 ± 2.3
Mat weight per cm^2 (mg)	1.6 ± 0.3	1.4 ± 0.3	1.5 ± 0.3	1.1 ± 0.1

Abbreviations: PEO (polyethylene oxide), CAM (chloramphenicol), LipCAM (chloramphenicol-loaded liposomes), SoyPC (phosphatidylcholine from soybeans).

3.3.3. Swelling index

To assess whether the incorporation of active ingredients affected the formulation's swelling capacity, swelling index in simulated wound fluid was repeated for the formulations containing the active ingredients. All formulations had a high swelling index and a high weight retained after the test (Fig. 9), as observed for Pectin-PEO before (Fig. 4A). That the weight retained after the test (close to 150 % for alle formulations) is higher than the initial weight (values over 100 %) (Fig. 4B) is probably due to the retention of salts from the simulated wound fluid in the fibers. The addition of CAM, LipCAM or CAM-SoyPC did not influence the swelling index, nor the weight retained after the test. Lanno et al., found that polycaprolactone (PCL) fibers loaded with CAM had a higher swelling index compared to that of pure PCL-fibers (Lanno et al., 2020), an observation that we did not see in our study. However, they postulated that this effect was due to the surface hydrophilization caused by the presence of CAM in the hydrophobic PCL fibers. In this study, the polymers used are very hydrophilic, hence we postulate that the addition of 2 % CAM and/or 10 % SoyPC did not affect the hydrophilicity of the fibers to the extent that the swelling behavior was changed.

3.3.4. In vitro chloramphenicol release

Sustained drug release from a wound dressing is desirable, as it reduces the need of dressing changes and thus increases patient comfort. CAM is a lipophilic compound that previously has been entrapped into liposomes for solubilization, stabilization and sustained CAM-release purposes from hydrogels (Ingebrigtsen et al., 2017a). Sustained release from nanofibers can be obtained by applying multiple strategies, including spinning of multilayer arrangement, co-axial electrospinning, post-spinning treatment (cross-linking) and by applying less water-soluble polymers (Gaydhane et al., 2023). However, the advantages of choosing liposomes-in-nanofiber formulations for this purpose, is that it 1) allows using biocompatible ingredients, including water-soluble polymers for fiber formation, and 2) allows avoiding toxic, organic solvents during electrospinning, that are often demanded for electrospinning of hydrophobic polymers (Casula et al., 2023).

The CAM-release was tested in a Franz diffusion set-up (as described in Section 2.8.5), comparing CAM-release from a solution made in PBS with CAM release from three different nanofibers (Fig. 10). As expected, the PBS-solution showed a very fast CAM release, with more than 80 % released within the first three hours. All nanofibers showed a sustained CAM release compared to the control during the first two hours (Fig. 10). Nevertheless, the nanofibers still displayed a burst CAM-release with around 60 % of the drug being released in the first two hours, which is a common release profile for nanofibers with small fiber diameters, and in compliance with drug release profiles normally seen from hydrophilic polymers (Krysiak and Stachewicz, 2022). This observed release profile can be considered ideal, since avoiding bacterial colonization in open fracture wounds has been observed to depend on a fast onset of the locally administered antibiotics (Burbank et al., 2020), suggesting a high dose of the antibiotic to the wound in the first hours is good for bacterial eradication. At the same time, frequent dressing changes are painful for the patient, and a dressing should therefore, in addition to a fast antibiotic onset, thus also be able to maintain an antibiotic concentration over a longer time. Nanofibers were therefore prepared with LipCAM containing both free and liposomal-entrapped CAM corresponding to the CAM-entrapment efficiency of 55 ± 9 % (Table 5) obtained during production. As can be seen in Fig. 10, the slowest CAM-release was obtained from Pectin-PEO-LipCAM with a statistically significant differences compared to Pectin-PEO-CAM after 0.5 and 1 h, indicate that liposomal-entrapped CAM has a delayed release from the nanofibers. However, Pectin-PEO-CAM-SoyPC, where CAM and phospholipids was added as separate solutions and not as preformed liposome dispersion, also led to a significantly slower release compared to Pectin-PEO-CAM, but just after 15 and 30 min of release. Both Pectin-PEO-LipCAM and Pectin-PEO-CAM-SoyPC showed a significantly more sustained CAM-

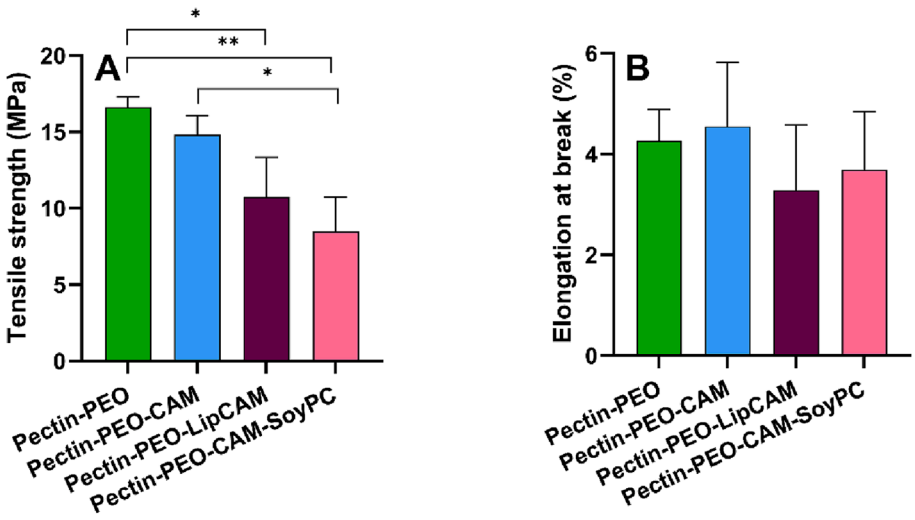

Fig. 8. Tensile strength (A) and elongation at break (B) of nanofibers. Results are presented as mean with their respective SD (n = 3). * $p < 0.05$, ** $p < 0.01$ Abbreviations: CAM (chloramphenicol), LipCAM (chloramphenicol-loaded liposomes), PEO (polyethylene oxide), SoyPC (phosphatidylcholine from soybeans).

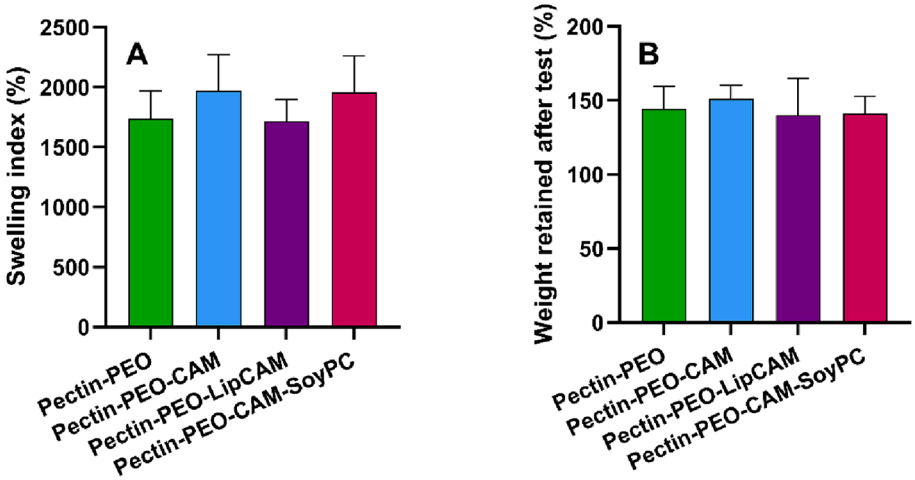

Fig. 9. Swelling behavior measured through swelling index (A) and weight retention after drying (B) of nanofibers of different complexity after exposure to simulated wound fluid (n = 3, results are presented as mean ± SD). Abbreviations: CAM (chloramphenicol), LipCAM (chloramphenicol-loaded liposomes), PEO (polyethylene oxide), SoyPC (phosphatidylcholine from soybeans).

release as compared to the control after four hours. Although the incorporation of free lipids together with free CAM into nanofibers also led to a slightly sustained release, maybe due to spontaneous vesicle formation or the more hydrophobic nature of the formed nanofibers, it seems like the preformation of LipCAM has a better and more reliable effect on sustaining drug release from pectin-PEO-nanofibers, and thus should be the preferred formulation.

Overall, our results show that incorporation of CAM into liposomes in pectin-PEO-nanofibers gives a slightly more sustained drug release.

3.3.5. *Cytotoxicity of nanofibers*

Considering the close contact with surrounding cells and tissues, biocompatibility is an important property of a wound dressing (Behere and Ingavle, 2021; Rani Raju et al., 2022). Dermal fibroblasts and macrophages (RAW 264.7) were chosen for *in vitro* cytotoxicity testing, due to the versatile and important role of both macrophages and fibroblasts in different stages of the wound healing process (Juncos Bombin et al., 2020).

Cells were treated with three different concentrations of each formulation: 125, 250 and 1000 μg/ml (Schulte-Werning et al., 2021) (Fig. 11). In the dermal fibroblasts the highest concentration of Pectin-PEO and Pectin-PEO-CAM showed a significantly reduced viability while the treatment with the highest concentrations of Pectin-PEO-LipCAM and Pectin-PEO-CAM-SoyPC lead to a significant but small elevation of the viability. A trend of increased cell viability was also observed on murine macrophages when treated with Pectin-PEO-LipCAM and Pectin-PEO-CAM-SoyPC, with no statistical significance. This could be explained by the presence of Lipoid S 100 (SoyPC) in liposomal form since a positive effect of empty liposomes comprising Lipoid S 100 on murine macrophages has been reported before (Hemmingsen et al., 2023). In general, all treatments led to a cell viability of over 90 % compared to the control and can thus be concluded to have no toxic effect on the cell viability of both cell lines (ISO, 2009). The polymers pectin and PEO are regarded as biocompatible (Filip and Peer, 2019; Han et al., 2022), which is supported by the lack of toxicity shown in our tests.

3.3.6. *Anti-inflammatory activity*

Inflammation is an essential part of the wound healing process (Rosique et al., 2015). However, difficult-to-heal wounds, like diabetic wounds, often show a persistent low-grade inflammation that leads to unwanted damage of normal tissue and can hinder the wound to process

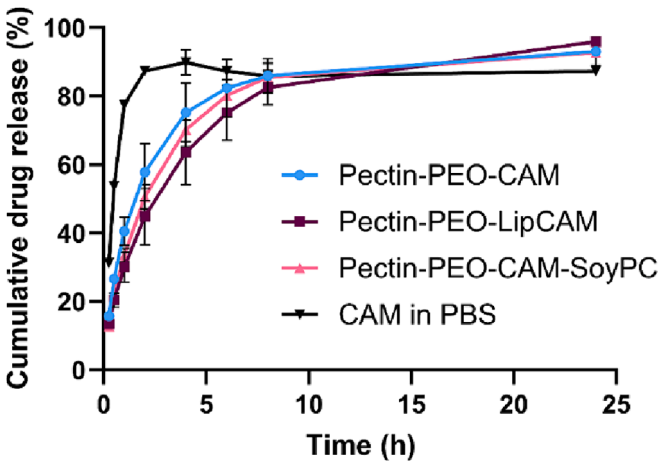

Fig. 10. Cumulative CAM release from nanofibers over 24 h presented as mean with their respective standard deviations, SD (n = 3). Abbreviations: CAM (chloramphenicol), LipCAM (chloramphenicol-loaded liposomes), PEO (polyethylene oxide), SoyPC (phosphatidylcholine from soybeans).

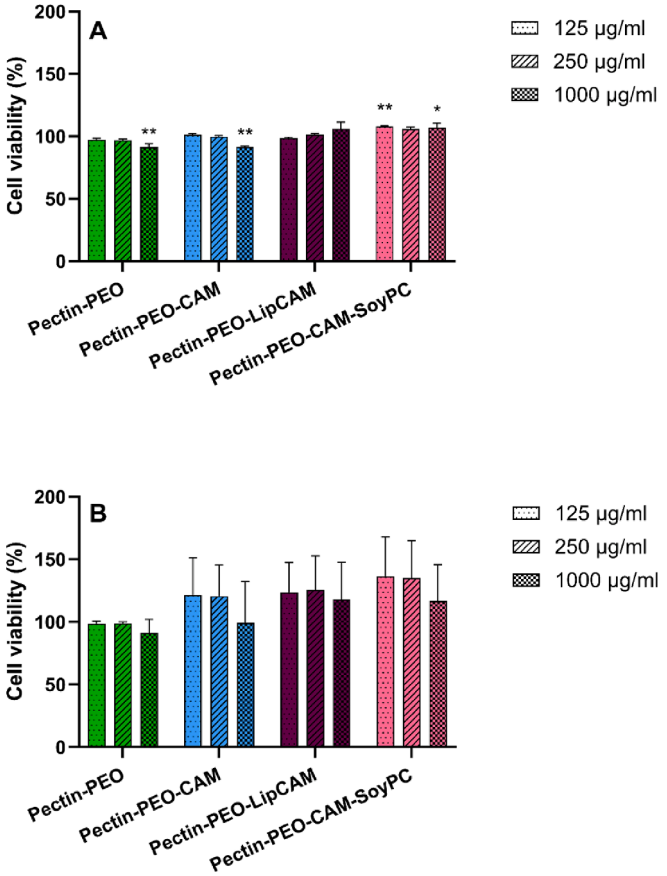

Fig. 11. Cytotoxicity of dermal fibroblasts (A) and murine macrophages (B) presented as mean with their respective SD (n = 3). * $p < 0.05$, ** $p < 0.01$, compared to control. Abbreviations: CAM (chloramphenicol), LipCAM (chloramphenicol-loaded liposomes), PEO (polyethylene oxide), SoyPC (phosphatidylcholine from soybeans).

into the next healing phase (Gao et al., 2022). Dressings containing anti-inflammatory drugs, might improve the healing outcome, as shown by Wang et al., who found that their hydrogels with vancomycin-conjugated silver nanoclusters with micelles that showed anti-inflammatory properties on LPS-inflamed macrophages also reduced the wound closure time in a diabetic mouse model (Wang et al., 2021).

In this study, we treated murine macrophages with LPS and our formulations and measured their inflammatory response by their production of nitric oxide (NO) (Fig. 12), a gasotransmitter, whose production is a characterization of pro-inflammatory macrophages (Roszer, 2015).

None of our nanofibers showed any increase in NO-production of the macrophages and thus no sign of an increased inflammatory activity. We have observed before that nanofibers with PEO did not show inflammatory activity on macrophages (Schulte-Werning et al., 2021). Pectin is reported to have some anti-inflammatory activity (Popov et al., 2013) and although we could see a reduction in NO production of macrophages treated with the highest concentration of Pectin-PEO, this was not significant (Fig. 12). However, the highest concentration (1000 µg/ml) of Pectin-PEO-CAM, Pectin-PEO-LipCAM and Pectin-PEO-CAM-SoyPC showed a significant reduction in NO production compared to the control (Fig. 12). This could be explained by the presence of SoyPC in the fibers since it has previously been shown that liposomes from Lipoid S 100 have a high potential in reducing the inflammation in LPS-induced macrophages (Cauzzo et al., 2020). These findings show that the nanofibers do not lead to an increased inflammatory response which could hamper the healing process but, in contrary, might be beneficial for the healing process due to their anti-inflammatory activity.

3.3.7. *Antimicrobial activity of nanofibers*

Nanofibers dry format makes them easy to handle and expands the storage of the formulations compared to hydrophilic wet formulations such as hydrogels. However, the fabrication technique requires a high voltage (80 kV), which might affect the incorporated antibiotic. To assess whether the dressings maintained the activity of CAM, we measured the antimicrobial activity of our nanofibers using a modified disc diffusion test with 30 µg CAM-discs as control. Since various bacterial species have found to be colonizing wounds, we chose two common species present in wounds: *S. aureus*, which is gram-positive, and *E. coli* as a gram-negative species (Buch et al., 2021).

No antimicrobial effect could be seen from Pectin-PEO on neither *E. coli* nor *S. aureus* (Fig. 13). This is in agreement with previous finding, where PEO-containing nanofibers prepared with different co-polymers also did not have any antimicrobial effect on the same two bacteria species (Schulte-Werning et al., 2021). All the prepared CAM-containing fibers, Pectin-PEO-CAM, Pectin-PEO-LipCAM and Pectin-PEO-CAM-SoyPC, showed a maintained antimicrobial effect on both tested species: *E. coli* and *S. aureus* as compared to the CAM control disc (Fig. 13). The marginal reduction seen for Pectin-PEO-CAM, Pectin-PEO-LipCAM

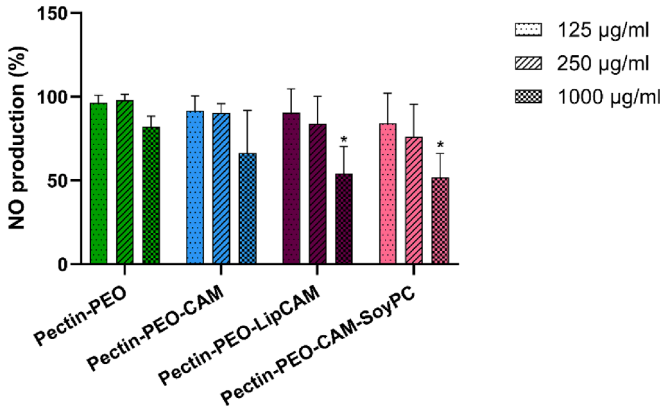

Fig. 12. NO production (%) of LPS treated macrophages (RAW 264.7 cells) exposed to different concentrations of nanofibers (125, 250 and 1000 µg/ml) for 24 h. Results are presented as mean with the respective standard deviations. * $p < 0.05$, compared to control. Abbreviations: Abbreviations: CAM (chloramphenicol), LipCAM (chloramphenicol-loaded liposomes), PEO (polyethylene oxide), SoyPC (phosphatidylcholine from soybeans).

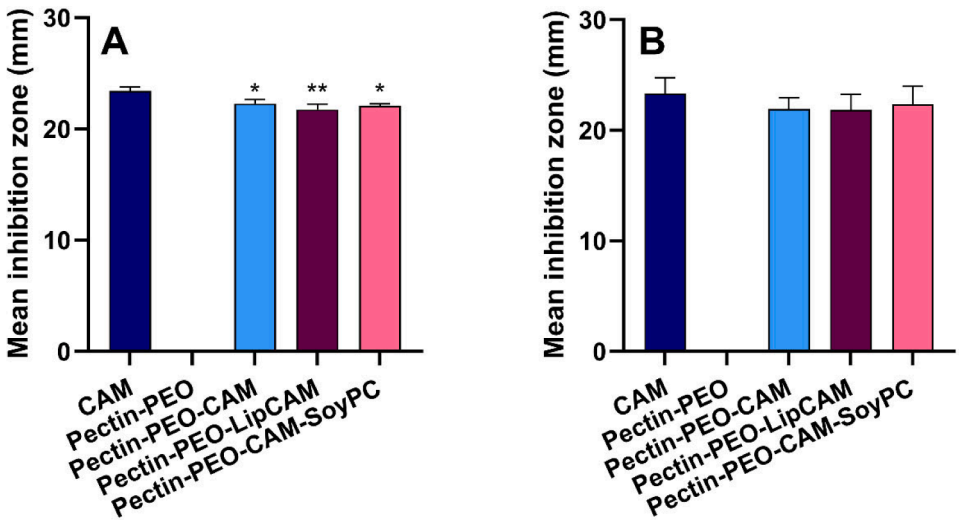

Fig. 13. Antimicrobial activity of nanofibers in E. coli (A) and S. aureus (B). Results are presented as mean inhibition zones with their respective standard deviations (n = 3). 30 μg CAM discs are used as positive control and CAM-free nanofibers (Pectin-PEO) as negative control. * $p < 0.05$, ** $p < 0.01$., compared to control. Abbreviations: CAM (chloramphenicol), LipCAM (chloramphenicol-loaded liposomes), PEO (polyethylene oxide), SoyPC (phosphatidylcholine from soybeans).

and Pectin-PEO-CAM-SoyPC as compared to the CAM control disc, with a slightly smaller inhibitions zones in *E. coli* (Fig. 13A), most probably is without any clinical relevance, but might be caused by a change in release properties. However, all nanofibers had a inhibition zones above 90 % of the inhibition zones of pure CAM (Fig. 13). Thus, nanofibers, including nanofibers with CAM entrapped into liposomes (LipCAM) did preserve CAMs' antimicrobial activity. It shows that although the nanofibers were produced in electrospinning with a high voltage (80 kV), intact CAM was maintained in the prepared nanofibers. Keeping in mind that nanofibers are dry formulations, it is also an excellent storage-format for CAM, known for its limited storage stability in aqueous formulations (Ingebrigtsen et al., 2017a).

4. Conclusion

Hydrophilic nanofibers from purely aqueous solutions were fabricated using the needle-free, wire-electrospinning technology. Pectin-PEO was the preferred polymer system considering its fast fiber deposition rate. We further demonstrated the successful incorporation of CAM in nanofibers, both when adding CAM directly to the polymer system, in preformed liposomes, as well as in dispersion with phospholipids. A more sustained CAM-release was observed in nanofibers *in vitro* as compared to the control CAM-solution, and especially with liposomes and phospholipids added to the nanofibers. But most importantly, a preserved antimicrobial effect close to pure CAM was maintained in all nanofibers, together with an elevated anti-inflammatory activity with phospholipids in the fibers, which makes the Pectin-PEO nanofiber formulation with CAM-liposomes a promising wound dressing for the future treatment of chronic wounds.

CRediT authorship contribution statement

Laura Victoria Schulte-Werning: Writing – original draft, Visualization, Validation, Methodology, Investigation, Funding acquisition, Formal analysis, Data curation, Conceptualization. **Bhupender Singh:** Writing – review & editing, Validation, Methodology. **Mona Johannessen:** Writing – review & editing, Validation, Supervision, Resources, Methodology. **Rolf Einar Engstad:** Writing – review & editing, Supervision, Resources, Methodology. **Ann Mari Holsæter:** Writing – review & editing, Writing – original draft, Supervision, Resources, Methodology, Funding acquisition, Conceptualization.

Declaration of competing interest

The authors declare that they have no known competing financial interests or personal relationships that could have appeared to influence the work reported in this paper.

Data availability

Data will be made available on request.

Acknowledgements

The publication charges for this article have been funded by the publication fund at UiT The Arctic University of Norway, Norway. The authors are grateful to Biotec BetaGlucans AS (Tromsø, Norway) for providing the Nanospider™. The authors would like to thank Lipoid GmbH (Ludwigshafen, Germany) for providing the phospholipids used in the experiments. The authors would also like to thank The Advanced Microscopy Core Facility, Department of Medical Biology, UiT The Arctic University of Norway for the assistance in SEM-imaging and Kenneth Bowitz Larsen at The Advanced Microscopy Core Facility, Department of Medical Biology, UiT The Arctic University of Norway for the assistance in confocal imaging.

References

Akombaetwa, N., Ilangala, A.B., Thom, L., Memvanga, P.B., Witika, B.A., Buya, A.B., 2023. Current Advances in Lipid Nanosystems Intended for Topical and Transdermal Drug Delivery Applications. Pharmaceutics 15, 656. https://doi.org/10.3390/pharmaceutics15020656.

Angammana, C.J., Jayaram, S.H., 2011. Analysis of the Effects of Solution Conductivity on Electrospinning Process and Fiber Morphology. IEEE Trans. Ind. Appl. 47, 1109–1117. https://doi.org/10.1109/tia.2011.2127431.

ASTM International, 2018. ASTM D882-18, Standard Test Method for Tensile Properties of Thin Plastic Sheeting. ASTM International, West Conshohocken, PA, US.

Aydogdu, A., Sumnu, G., Sahin, S., 2018. A novel electrospun hydroxypropyl methylcellulose/polyethylene oxide blend nanofibers: Morphology and physicochemical properties. Carbohydr. Polym. 181, 234–246. https://doi.org/10.1016/j.carbpol.2017.10.071.

Behere, I., Ingavle, G., 2021. In vitro and in vivo advancement of multifunctional electrospun nanofiber scaffolds in wound healing applications: Innovative nanofiber designs, stem cell approaches, and future perspectives. J. Biomed. Mater. Res. A 110, 443–461. https://doi.org/10.1002/jbm.a.37290.

Blanco-Fernandez, B., Castano, O., Mateos-Timoneda, M.A., Engel, E., Pérez-Amodio, S., 2021. Nanotechnology Approaches in Chronic Wound Healing. Adv. Wound Care (new Rochelle) 10, 234–256. https://doi.org/10.1089/wound.2019.1094.

Bradford, C., Freeman, R., Percival, S.L., 2009. In Vitro Study of Sustained Antimicrobial Activity of a New Silver Alginate Dressing. J. Am. Col. Certif. Wound Spec. 1, 117–120. https://doi.org/10.1016/j.jcws.2009.09.001.

Brennan, M.B., Hess, T.M., Bartle, B., Cooper, J.M., Kang, J., Huang, E.S., Smith, M., Sohn, M.W., Crnich, C., 2017. Diabetic foot ulcer severity predicts mortality among veterans with type 2 diabetes. J. Diabetes Complicat. 31, 556–561. https://doi.org/10.1016/j.jdiacomp.2016.11.020.

Buch, P.J., Chai, Y., Goluch, E.D., 2021. Bacterial chatter in chronic wound infections. Wound Repair Regen. 29, 106–116. https://doi.org/10.1111/wrr.12867.

Burbank, K.M., Schauer, S.G., De Lorenzo, R.A., Wenke, J.C., 2020. Early application of topical antibiotic powder in open-fracture wounds: A strategy to prevent biofilm formation and infections. OTA International 3, e091.

Casula, L., Zidar, A., Kristl, J., Jeras, M., Kralj, S., Fadda, A.M., Zupančič, S., 2023. Development of Nanofibers with Embedded Liposomes Containing an Immunomodulatory Drug Using Green Electrospinning. Pharmaceutics 15, 1245. https://doi.org/10.3390/pharmaceutics15041245.

Cauzzo, J., Nystad, M., Holsæter, A.M., Basnet, P., Škalko-Basnet, N., 2020. Following the Fate of Dye-Containing Liposomes In Vitro. Int. J. Mol. Sci. 21 https://doi.org/10.3390/ijms21144847.

Chandrawati, R., Olesen, M.T.J., Marini, T.C.C., Bisra, G., Guex, A.G., de Oliveira, M.G., Zelikin, A.N., Stevens, M.M., 2017. Enzyme Prodrug Therapy Engineered into Electrospun Fibers with Embedded Liposomes for Controlled, Localized Synthesis of Therapeutics. Adv. Healthc. Mater. 6, 1700385. https://doi.org/10.1002/adhm.201700385.

Cui, S., Yao, B., Sun, X., Hu, J., Zhou, Y., Liu, Y., 2016. Reducing the content of carrier polymer in pectin nanofibers by electrospinning at low loading followed with selective washing. Mater. Sci. Eng. C 59, 885–893. https://doi.org/10.1016/j.msec.2015.10.086.

Cui, Z., Zheng, Z., Lin, L., Si, J., Wang, Q., Peng, X., Chen, W., 2018. Electrospinning and crosslinking of polyvinyl alcohol/chitosan composite nanofiber for transdermal drug delivery. Adv. Polym. Technol. 37, 1917–1928. https://doi.org/10.1002/adv.21850.

Elmarco, 2023. Patented needle-free NanospiderTM technology. https://www.elmarco.com/nanospider (accessed 6 December 2023).

Fareed, F., Saeed, F., Afzaal, M., Imran, A., Ahmad, A., Mahmood, K., Shah, Y.A., Hussain, M., Ateeq, H., 2022. Fabrication of electrospun gum Arabic-polyvinyl alcohol blend nanofibers for improved viability of the probiotic. J. Food Sci. Technol. 59, 4812–4821. https://doi.org/10.1007/s13197-022-05567-1.

Filip, P., Peer, P., 2019. Characterization of Poly(Ethylene Oxide) Nanofibers—Mutual Relations between Mean Diameter of Electrospun Nanofibers and Solution Characteristics. Processes 7. https://doi.org/10.3390/pr7120948.

Frantz, C., Stewart, K.M., Weaver, V.M., 2010. The extracellular matrix at a glance. J. Cell Sci. 123, 4195–4200. https://doi.org/10.1242/jcs.023820.

Gao, Z., Wang, Q., Yao, Q., Zhang, P., 2022. Application of Electrospun Nanofiber Membrane in the Treatment of Diabetic Wounds. Pharmaceutics 14, 6. https://doi.org/10.3390/pharmaceutics14010006.

Gaydhane, M.K., Sharma, C.S., Majumdar, S., 2023. Electrospun nanofibres in drug delivery: advances in controlled release strategies. RSC Adv. 13, 7312–7328. https://doi.org/10.1039/d2ra06023j.

Ge, Y., Tang, J., Fu, H., Fu, Y., Wu, Y., 2019. Characteristics, Controlled-release and Antimicrobial Properties of Tea Tree Oil Liposomes-incorporated Chitosan-based Electrospun Nanofiber Mats. Fibers Polym. 20, 698–708. https://doi.org/10.1007/s12221-019-1092-1.

Gómez-Mascaraque, L.G., Casagrande Sipoli, C., de La Torre, L.G., López-Rubio, A., 2017. Microencapsulation structures based on protein-coated liposomes obtained through electrospraying for the stabilization and improved bioaccessibility of curcumin. Food Chem. 233, 343–350. https://doi.org/10.1016/j.foodchem.2017.04.133.

Graves, N., Phillips, C.J., Harding, K., 2022. A narrative review of the epidemiology and economics of chronic wounds. Br. J. Dermatol. 187, 141–148. https://doi.org/10.1111/bjd.20692.

Grip, J., Engstad, R.E., Skjaeveland, I., Škalko-Basnet, N., Isaksson, J., Basnet, P., Holsæter, A.M., 2018. Beta-glucan-loaded nanofiber dressing improves wound healing in diabetic mice. Eur. J. Pharm. Sci. 121, 269–280. https://doi.org/10.1016/j.ejps.2018.05.031.

Haider, A., Haider, S., Kang, I.-K., 2018. A comprehensive review summarizing the effect of electrospinning parameters and potential applications of nanofibers in biomedical and biotechnology. Arab. J. Chem. 11, 1165–1188. https://doi.org/10.1016/j.arabjc.2015.11.015.

Han, S.S., Ji, S.M., Park, M.J., Suneetha, M., Uthappa, U.T., 2022. Pectin Based Hydrogels for Drug Delivery Applications: A Mini Review. Gels 8. https://doi.org/10.3390/gels8120834.

Hasan, S., Hasan, M.A., Hassan, M.U., Amin, M., Javed, T., Fatima, L., 2023. Biopolymers in diabetic wound care management: A potential substitute to traditional dressings. Eur. Polym. J. 189 https://doi.org/10.1016/j.eurpolymj.2023.111979.

Hasanbegloo, K., Banihashem, S., Faraji Dizaji, B., Bybordi, S., Farrokh-Eslamlou, N., Abadi, P.G., Jazi, F.S., Irani, M., 2023. Paclitaxel-loaded liposome-incorporated chitosan (core)/poly(epsilon-caprolactone)/chitosan (shell) nanofibers for the treatment of breast cancer. Int. J. Biol. Macromol. 230, 123380. https://doi.org/10.1016/j.ijbiomac.2023.123380.

Hemmingsen, L.M., Giordani, B., Paulsen, M.H., Vanić, Ž., Flaten, G.E., Vitali, B., Basnet, P., Bayer, A., Strøm, M.B., Škalko-Basnet, N., 2023. Tailored anti-biofilm activity – Liposomal delivery for mimic of small antimicrobial peptide. Biomater. Adv. 145, 213238. https://doi.org/10.1016/j.bioadv.2022.213238.

Holsæter, A.M., Wizgird, K., Karlsen, I., Hemmingsen, J.F., Brandl, M., Škalko-Basnet, N., 2022. How docetaxel entrapment, vesicle size, zeta potential and stability change with liposome composition-A formulation screening study. Eur. J. Pharm. Sci. 177, 106267. https://doi.org/10.1016/j.ejps.2022.106267.

Homaeigohar, S., Boccaccini, A.R., 2020. Antibacterial biohybrid nanofibers for wound dressings. Acta Biomater. 107, 25–49. https://doi.org/10.1016/j.actbio.2020.02.022.

Ingebrigtsen, S.G., Didriksen, A., Johannessen, M., Škalko-Basnet, N., Holsæter, A.M., 2017a. Old drug, new wrapping - A possible comeback for chloramphenicol? Int. J. Pharm. 526, 538–546. https://doi.org/10.1016/j.ijpharm.2017.05.025.

Ingebrigtsen, S.G., Škalko-Basnet, N., de Albuquerque Cavalcanti Jacobsen, C., Holsæter, A.M, 2017b. Successful co-encapsulation of benzoyl peroxide and chloramphenicol in liposomes by a novel manufacturing method - dual asymmetric centrifugation. Eur. J. Pharm. Sci. 97, 192–199. https://doi.org/10.1016/j.ejps.2016.11.017.

ISO, I.O.f.S., 2009. ISO 10993-5:2009 Biological evaluation of medical devices - Part 5: Tests for in vitro cytotoxicity.

Juncos Bombin, A.D., Dunne, N.J., McCarthy, H.O., 2020. Electrospinning of natural polymers for the production of nanofibres for wound healing applications. Mater. Sci. Eng. C 114. https://doi.org/10.1016/j.msec.2020.110994.

Kajdič, S., Planinšek, O., Gašperlin, M., Kocbek, P., 2019. Electrospun nanofibers for customized drug-delivery systems. J. Drug Deliv. Sci. Technol. 51, 672–681. https://doi.org/10.1016/j.jddst.2019.03.038.

Kim, H.H., Kim, M.J., Ryu, S.J., Ki, C.S., Park, Y.H., 2016. Effect of fiber diameter on surface morphology, mechanical property, and cell behavior of electrospun poly (ε-caprolactone) mat. Fibers Polym. 17, 1033–1042. https://doi.org/10.1007/s12221-016-6350-x.

Kowalski, G., Kijowska, K., Witczak, M., Kuterasinski, L., Lukasiewicz, M., 2019. Synthesis and Effect of Structure on Swelling Properties of Hydrogels Based on High Methylated Pectin and Acrylic Polymers. Polymers (basel) 11. https://doi.org/10.3390/polym11010114.

Krysiak, Z.J., Stachewicz, U., 2022. Electrospun fibers as carriers for topical drug delivery and release in skin bandages and patches for atopic dermatitis treatment. Wiley Interdiscip. Rev. Nanomed. Nanobiotechnol. 15, e1829.

Lanno, G.M., Ramos, C., Preem, L., Putrins, M., Laidmae, I., Tenson, T., Kogermann, K., 2020. Antibacterial Porous Electrospun Fibers as Skin Scaffolds for Wound Healing Applications. ACS Omega 5, 30011–30022. https://doi.org/10.1021/acsomega.0c04402.

Li, Z., Kang, H., Li, Q., Che, N., Liu, Z., Li, P., Zhang, C., Liu, R., Huang, Y., 2014. Ultrathin core-sheath fibers for liposome stabilization. Colloids Surf. B 122, 630–637. https://doi.org/10.1016/j.colsurfb.2014.07.042.

Li, D.-Q., Li, J., Dong, H.-L., Li, X., Zhang, J.-Q., Ramaswamy, S., Xu, F., 2021. Pectin in biomedical and drug delivery applications: A review. Int. J. Biol. Macromol. 185, 49–65. https://doi.org/10.1016/j.ijbiomac.2021.06.088.

Li, K., Zhu, Z., Zhai, Y., Chen, S., 2023. Recent Advances in Electrospun Nanofiber-Based Strategies for Diabetic Wound Healing Application. Pharmaceutics 15. https://doi.org/10.3390/pharmaceutics15092285.

Mašková, E., Kubová, K., Raimi-Abraham, B.T., Vllasaliu, D., Vohlídalová, E., Turánek, J., Mašek, J., 2020. Hypromellose – A traditional pharmaceutical excipient with modern applications in oral and oromucosal drug delivery. J. Control. Release 324, 695–727. https://doi.org/10.1016/j.jconrel.2020.05.045.

Mickova, A., Buzgo, M., Benada, O., Rampichova, M., Fisar, Z., Filova, E., Tesarova, M., Lukas, D., Amler, E., 2012. Core/Shell Nanofibers with Embedded Liposomes as a Drug Delivery System. Biomacromolecules 13, 952–962. https://doi.org/10.1021/bm2018118.

Mohnen, D., 2008. Pectin structure and biosynthesis. Curr. Opin. Plant Biol. 11, 266–277. https://doi.org/10.1016/j.pbi.2008.03.006.

Olechno, K., Grilc, N.K., Zupančič, S., Winnicka, K., 2022. Incorporation of Ethylcellulose Microparticles Containing a Model Drug with a Bitter Taste into Nanofibrous Mats by the Electrospinning Technique-Preliminary Studies. Materials (basel) 15. https://doi.org/10.3390/ma15155286.

Olsson, M., Jarbrink, K., Divakar, U., Bajpai, R., Upton, Z., Schmidtchen, A., Car, J., 2019. The humanistic and economic burden of chronic wounds: A systematic review. Wound Repair Regen. 27, 114–125. https://doi.org/10.1111/wrr.12683.

Park, J.-C., Ito, T., Kim, K.-O., Kim, K.-W., Kim, B.-S., Khil, M.-S., Kim, H.-Y., Kim, I.-S., 2010. Electrospun poly(vinyl alcohol) nanofibers: effects of degree of hydrolysis and enhanced water stability. Polym. J. 42, 273–276. https://doi.org/10.1038/pj.2009.340.

Pillay, V., Dott, C., Choonara, Y.E., Tyagi, C., Tomar, L., Kumar, P., du Toit, L.C., Ndesendo, V.M.K., 2013. A Review of the Effect of Processing Variables on the Fabrication of Electrospun Nanofibers for Drug Delivery Applications. J. Nanomater. 2013, 1–22. https://doi.org/10.1155/2013/789289.

Pires, F., Santos, J.F., Bitoque, D., Silva, G.A., Marletta, A., Nunes, V.A., Ribeiro, P.A., Silva, J.C., Raposo, M., 2019. Polycaprolactone/Gelatin Nanofiber Membranes Containing EGCG-Loaded Liposomes and Their Potential Use for Skin Regeneration. ACS Appl. Bio Mater. 2, 4790–4800. https://doi.org/10.1021/acsabm.9b00524.

Popov, S.V., Markov, P.A., Popova, G.Y., Nikitina, I.R., Efimova, L., Ovodov, Y.S., 2013. Anti-inflammatory activity of low and high methoxylated citrus pectins. Biomed. Prev. Nutr. 3, 59–63. https://doi.org/10.1016/j.bionut.2012.10.008.

Ramakrishnan, R., Gimbun, J., Ramakrishnan, P., Ranganathan, B., Reddy, S.M.M., Shanmugam, G., 2019. Effect of Solution Properties and Operating Parameters on Needleless Electrospinning of Poly(Ethylene Oxide) Nanofibers Loaded with Bovine Serum Albumin. Curr. Drug Deliv. 16 https://doi.org/10.2174/1567201816666191029122445.

Rani Raju, N., Silina, E., Stupin, V., Manturova, N., Chidambaram, S.B., Achar, R.R., 2022. Multifunctional and Smart Wound Dressings-A Review on Recent Research Advancements in Skin Regenerative Medicine. Pharmaceutics 14. https://doi.org/10.3390/pharmaceutics14081574.

Rasband, W.S., 1997-2018. ImageJ. National Institutes of Health, Bethesda, Maryland, USA.

Reneker, D.H., Yarin, A.L., 2008. Electrospinning jets and polymer nanofibers. Polymer 49, 2387–2425. https://doi.org/10.1016/j.polymer.2008.02.002.
Rockwell, P.L., Kiechel, M.A., Atchison, J.S., Toth, L.J., Schauer, C.L., 2014. Various-sourced pectin and polyethylene oxide electrospun fibers. Carbohydr. Polym. 107, 110–118. https://doi.org/10.1016/j.carbpol.2014.02.026.
Rosique, R.G., Rosique, M.J., Farina Junior, J.A., 2015. Curbing Inflammation in Skin Wound Healing: A Review. Int. J. Inflam. 2015, 316235. https://doi.org/10.1155/2015/316235.
Roszer, T., 2015. Understanding the Mysterious M2 Macrophage through Activation Markers and Effector Mechanisms. Mediators Inflamm. 2015, 816460. https://doi.org/10.1155/2015/816460.
Schindelin, J., Arganda-Carreras, I., Frise, E., Kaynig, V., Longair, M., Pietzsch, T., Preibisch, S., Rueden, C., Saalfeld, S., Schmid, B., Tinevez, J.Y., White, D.J., Hartenstein, V., Eliceiri, K., Tomancak, P., Cardona, A., 2012. Fiji: an open-source platform for biological-image analysis. Nat. Methods 9, 676–682. https://doi.org/10.1038/nmeth.2019.
Schulte-Werning, L.V., Murugaiah, A., Singh, B., Johannessen, M., Engstad, R.E., Škalko-Basnet, N., Holsæter, A.M., 2021. Multifunctional Nanofibrous Dressing with Antimicrobial and Anti-Inflammatory Properties Prepared by Needle-Free Electrospinning. Pharmaceutics 13, 1527. https://doi.org/10.3390/pharmaceutics13091527.
Sen, C.K., 2021. Human Wound and Its Burden: Updated 2020 Compendium of Estimates. Adv. Wound Care (new Rochelle) 10, 281–292. https://doi.org/10.1089/wound.2021.0026.
Shihan, M.H., Novo, S.G., Le Marchand, S.J., Wang, Y., Duncan, M.K., 2021. A simple method for quantitating confocal fluorescent images. Biochem. Biophys. Rep. 25, 100916 https://doi.org/10.1016/j.bbrep.2021.100916.
Smistad, G., Bøyum, S., Alund, S.J., Samuelsen, A.B., Hiorth, M., 2012. The potential of pectin as a stabilizer for liposomal drug delivery systems. Carbohydr. Polym. 90, 1337–1344. https://doi.org/10.1016/j.carbpol.2012.07.002.
Stie, M.B., Jones, M., Sorensen, H.O., Jacobsen, J., Chronakis, I.S., Nielsen, H.M., 2019. Acids 'generally recognized as safe' affect morphology and biocompatibility of electrospun chitosan/polyethylene oxide nanofibers. Carbohydr. Polym. 215, 253–262. https://doi.org/10.1016/j.carbpol.2019.03.061.
Ternullo, S., de Weerd, L., Holsæter, A.M., Flaten, G.E., Skalko-Basnet, N., 2017. Going skin deep: A direct comparison of penetration potential of lipid-based nanovesicles on the isolated perfused human skin flap model. Eur. J. Pharm. Biopharm. 121, 14–23. https://doi.org/10.1016/j.ejpb.2017.09.006.
Thakkar, S., Misra, M., 2017. Electrospun polymeric nanofibers: New horizons in drug delivery. Eur. J. Pharm. Sci. 107, 148–167. https://doi.org/10.1016/j.ejps.2017.07.001.
Uhljar, L.É., Ambrus, R., 2023. Electrospinning of Potential Medical Devices (Wound Dressings, Tissue Engineering Scaffolds, Face Masks) and Their Regulatory Approach. Pharmaceutics 15. https://doi.org/10.3390/pharmaceutics15020417.
Vass, P., Szabo, E., Domokos, A., Hirsch, E., Galata, D., Farkas, B., Demuth, B., Andersen, S.K., Vigh, T., Verreck, G., Marosi, G., Nagy, Z.K., 2020. Scale-up of electrospinning technology: Applications in the pharmaceutical industry. Wiley Interdiscip. Rev. Nanomed. Nanobiotechnol. 12, e1611.
Verma, D.D., Verma, S., Blume, G., Fahr, A., 2003. Particle size of liposomes influences dermal delivery of substances into skin. Int. J. Pharm. 258, 141–151. https://doi.org/10.1016/s0378-5173(03)00183-2.
Wang, Y., Wu, Y., Long, L., Yang, L., Fu, D., Hu, C., Kong, Q., Wang, Y., 2021. Inflammation-Responsive Drug-Loaded Hydrogels with Sequential Hemostasis, Antibacterial, and Anti-Inflammatory Behavior for Chronically Infected Diabetic Wound Treatment. ACS Appl. Mater. Interfaces 13, 33584–33599. https://doi.org/10.1021/acsami.1c09889.
Xu, C., Ma, J., Wang, W., Liu, Z., Gu, L., Qian, S., Hou, J., Jiang, Z., 2022. Preparation of pectin-based nanofibers encapsulating Lactobacillus rhamnosus 1.0320 by electrospinning. Food Hydrocoll. 124 https://doi.org/10.1016/j.foodhyd.2021.107216.
Yalcinkaya, F., 2017. Preparation of various nanofiber layers using wire electrospinning system. Arab. J. Chem. 12, 5162–5172. https://doi.org/10.1016/j.arabjc.2016.12.012.
Yu, D.-G., Branford-White, C., Williams, G.R., Bligh, S.W.A., White, K., Zhu, L.-M., Chatterton, N.P., 2011. Self-assembled liposomes from amphiphilic electrospun nanofibers. Soft Matter 7, 8239–8247. https://doi.org/10.1039/c1sm05961k.